OPEN ACCESS Freely available online

PLoS one

C/EBPβ Promotes Transition from Proliferation to Hypertrophic Differentiation of Chondrocytes through Transactivation of $p57^{Kip2}$

Makoto Hirata[1☯], Fumitaka Kugimiya[1☯], Atsushi Fukai[1], Shinsuke Ohba[2], Naohiro Kawamura[1], Toru Ogasawara[1], Yosuke Kawasaki[1], Taku Saito[1], Fumiko Yano[2], Toshiyuki Ikeda[1], Kozo Nakamura[1], Ung-il Chung[2], Hiroshi Kawaguchi[1]*

1 Departments of Sensory & Motor System Medicine, Faculty of Medicine, University of Tokyo, Bunkyo-ku, Tokyo, Japan, 2 Center for Disease Biology and Integrative Medicine, Faculty of Medicine, University of Tokyo, Bunkyo-ku, Tokyo, Japan

Abstract

Background: Although transition from proliferation to hypertrophic differentiation of chondrocytes is a crucial step for endochondral ossification in physiological skeletal growth and pathological disorders like osteoarthritis, the underlying mechanism remains an enigma. This study investigated the role of the transcription factor CCAAT/enhancer-binding protein β (C/EBPβ) in chondrocytes during endochondral ossification.

Methodology/Principal Findings: Mouse embryos with homozygous deficiency in C/EBPβ (C/EBPβ−/−) exhibited dwarfism with elongated proliferative zone and delayed chondrocyte hypertrophy in the growth plate cartilage. In the cultures of primary C/EBPβ−/− chondrocytes, cell proliferation was enhanced while hypertrophic differentiation was suppressed. Contrarily, retroviral overexpression of C/EBPβ in chondrocytes suppressed the proliferation and enhanced the hypertrophy, suggesting the cell cycle arrest by C/EBPβ. In fact, a DNA cell cycle histogram revealed that the C/EBPβ overexpression caused accumulation of cells in the G0/G1 fraction. Among cell cycle factors, microarray and real-time RT-PCR analyses have identified the cyclin-dependent kinase inhibitor $p57^{Kip2}$ as the transcriptional target of C/EBPβ. $p57^{Kip2}$ was co-localized with C/EBPβ in late proliferative and pre-hypertrophic chondrocytes of the mouse growth plate, which was decreased by the C/EBPβ deficiency. Luciferase-reporter and electrophoretic mobility shift assays identified the core responsive element of C/EBPβ in the $p57^{Kip2}$ promoter between −150 and −130 bp region containing a putative C/EBP motif. The knockdown of $p57^{Kip2}$ by the siRNA inhibited the C/EBPβ-induced chondrocyte hypertrophy. Finally, when we created the experimental osteoarthritis model by inducing instability in the knee joints of adult mice of wild-type and C/EBPβ+/− littermates, the C/EBPβ insufficiency caused resistance to joint cartilage destruction.

Conclusions/Significance: C/EBPβ transactivates $p57^{Kip2}$ to promote transition from proliferation to hypertrophic differentiation of chondrocytes during endochondral ossification, suggesting that the C/EBPβ-$p57^{Kip2}$ signal would be a therapeutic target of skeletal disorders like growth retardation and osteoarthritis.

Citation: Hirata M, Kugimiya F, Fukai A, Ohba S, Kawamura N, et al. (2009) C/EBPβ Promotes Transition from Proliferation to Hypertrophic Differentiation of Chondrocytes through Transactivation of $p57^{Kip2}$. PLoS ONE 4(2): e4543. doi:10.1371/journal.pone.0004543

Editor: Thomas Zwaka, Baylor College of Medicine, United States of America

Received September 29, 2008; **Accepted** January 6, 2009; **Published** February 20, 2009

Funding: This study was supported by a Grant-in-aid for Scientific Research from the Japanese Ministry of Education, Culture, Sports, Science, and Technology (#19109007). The sponsor had no role in study design, data collection, data analysis, data interpretation, or writing of the manuscript.

Competing Interests: The authors have declared that no competing interests exist.

* E-mail: kawaguchi-ort@h.u-tokyo.ac.jp

☯ These authors contributed equally to this work.

Introduction

Most skeletal growth is achieved by endochondral ossification. During the process, chondrocytes undergo proliferation, hypertrophic differentiation, and apoptosis [1], each of which is regulated by distinct signals. Among them, chondrocyte hypertrophy is a rate-limiting step for the skeletal growth, being responsible for 40–60% of the endochondral ossification [2,3]. The initiation is precisely linked with the cessation of proliferation; however, the molecular mechanism underlying the harmonious transition from the proliferation to hypertrophic differentiation of chondrocytes remains an enigma.

CCAAT/enhancer-binding protein β (C/EBPβ), also known as nuclear factor-interleukin-6 (NF-IL6), is a member of the C/EBP family of six transcription factors characterized by a carboxyl-terminal leucine zipper dimerization domain and an adjacent highly conserved basic DNA binding domain [4–6]. Contrary to C/EBPα that is purely antiproliferative as a tumor suppressor in several cell types, C/EBPβ regulates expression of various genes involved in cell differentiation, proliferation, survival, immune function and female reproduction, as well as tumor invasiveness and progression, through a variety of mechanisms [6].Over the past several years, C/EBPβ has been shown to control differentiation of hematopoietic and adipogenic cells [7,8]. The

present study initially investigated skeletal phenotype of C/EBPβ-deficient (C/EBPβ−/−) mice which have been reported to display mainly hematopoietic and adipogenic defects [9–11]. The mice showed dwarfism with an elongated proliferative zone and delayed chondrocyte hypertrophy in the limb cartilage, implicating the cell cycle control by C/EBPβ in chondrocytes.

Cell cycle factors appear to play an important role in the control of chondrocyte proliferation and differentiation [12,13]. During the cell cycle activation, complexes of cyclin and cyclin-dependent kinase (CDK) promote G1/S-phase transition from G0/G1 by phosphorylating Rb-related pocket proteins, which activate genes required for the S-phase entry. The cyclin-CDK complexes are inhibited by two major families of CDK inhibitors [14]. The p16 INK4 family specifically binds and inactivates monomeric CDK4 or CDK6, whereas the Cip/Kip family, which includes $p21^{Cip1}$, $p27^{Kip1}$, and $p57^{Kip2}$ (p57), inhibits all G1/S-phase cyclin-CDK complexes. Since the control of these cell cycle factors driving S-phase onset greatly influences the commitment to cell differentiation, the present study performed a screen of potential transcriptional targets of C/EBPβ using a microarray analysis, and identified p57 as the most probable target during hypertrophic differentiation of chondrocytes. We further investigated the molecular mechanism underlying the regulation of skeletal growth and endochondral ossification through the C/EBPβ-p57 signal in chondrocytes.

Results

C/EBPβ−/− mice exhibit impaired skeletal growth and endochondral ossification

To analyze the physiological role of C/EBPβ in skeletal growth and endochondral ossification, we investigated the skeletal phenotypes of heterozygous and homozygous C/EBPβ-deficient (C/EBPβ+/− and C/EBPβ−/−) mice. Although the C/EBPβ+/− skeleton was normal, C/EBPβ−/− mice exhibited dwarfism as compared to the wild-type littermates from embryonic stages (Figure 1A). After birth, however, the skeletal size of C/EBPβ−/− mice gradually caught up with that of the wild type littermates (Figure 1B), and they became similar after 1 week of age. At the embryos, the limbs and vertebrae which are known to be primarily formed through endochondral ossification were about 20–25% shorter in C/EBPβ−/− mice than the wild-type, although calvarial growth, especially the width, formed through endochondral ossification and intramembranous ossification did not show such a difference (Figure 1D). Skeletal double staining revealed that not only the total bone length, but also the ratio of mineralized area shown by the positive Alizarin red staining to the total length was decreased, confirming that endochondral ossification was impaired by the C/EBPβ deficiency (Figure 1C, E).

Hypertrophic differentiation of chondrocytes is delayed in the C/EBPβ−/− limb cartilage

To know the mechanism underlying the impaired skeletal growth in C/EBPβ−/− mice, we compared the tibial limb cartilage of the wild-type and C/EBPβ−/− littermates at E16.5 (Figure 2A). Among the resting, proliferative, hypertrophic zones, and bone area, the proliferative zone was elongated while the hypertrophic zone was normal in the C/EBPβ−/− limb (Figure 2B). The number of proliferating chondrocytes with BrdU uptake was actually increased in the C/EBPβ−/− cartilage (Figure 2C).

C/EBPβ was shown by immunohistochemistry to be localized predominantly in late proliferative and pre-hypertrophic chondrocytes of the wild-type cartilage, but not in the C/EBPβ−/− cartilage (Figure 2D, top). Further histological examination by BrdU labeling, in situ hybridization of type X collagen (COL10), immunohistochemistry of indian hedgehog (Ihh), and Alcian blue/von Kossa double stainings supported the elongation of the proliferative zone and delay of chondrocyte hypertrophy by the C/EBPβ deficiency (Figure 2D).

C/EBPβ inhibits proliferation and promotes hypertrophic differentiation in cultured primary chondrocytes

When primary chondrocytes derived from mouse ribs and mouse chondrogenic cell line ATDC5 were cultured in the differentiation medium, the C/EBPβ mRNA level was increased with the differentiation (Figure 3A), which was comparable to the in vivo expression pattern of the limb cartilage.

We then examined the effects of loss- and gain-of-functions of C/EBPβ on proliferation and hypertrophic differentiation of the primary rib chondrocytes. When chondrocytes from wild-type and C/EBPβ−/− littermates were compared, cell number determined by the XTT assay was enhanced in the C/EBPβ−/− chondrocytes at 3 d of culture (Figure 3B). The percentage of BrdU-positive cells was also increased in the C/EBPβ−/− culture at this time point (Figure 3C), indicating that the increased cell number was due to the enhanced proliferation, rather than the effect on cell survival, vitality, or apoptosis. Contrarily, hypertrophic differentiation determined by alkaline phosphatase (ALP) and Alizarin red stainings, and mRNA levels of COL10, matrix metalloproteinase-13 (MMP13) and vascular endothelial growth factor (VEGF), parameters of chondrocyte hypertrophy, were suppressed by the deficiency (Figure 3D).

In contrast, retroviral overexpression of C/EBPβ in the wild-type rib chondrocytes suppressed the proliferation and enhanced the hypertrophic differentiation parameters (Figure 3E, F, and G). Collectively, C/EBPβ was shown to be essential for cessation of proliferation and promotion of hypertrophic differentiation, suggesting arrest of the cell cycle and exit from it.

C/EBPβ regulates cell cycle and p57 as the transcriptional target

We therefore examined the regulation of cell cycle by C/EBPβ. A DNA cell cycle histogram in mouse mesenchymal C3H10T1/2 cells after the cycle synchronization revealed that the C/EBPβ overexpression enhanced accumulation of cells in the G0/G1 fraction (Figure 4A). To identify cell cycle factors lying downstream of the C/EBPβ signal, we performed a screen of transcriptional targets of C/EBPβ using a microarray analysis (Table S1). The C/EBPβ overexpression caused downregulation of cyclin B1, B2 and D1, and upregulation of the cyclin-dependent kinase inhibitors p16, p21 and p57, by 50% or more as compared to the empty vector overexpression. Since the above analyses were performed in non-chondrogenic C3H10T1/2 cells, we further examined the expressions of the candidate genes by real-time RT-PCR analysis in the cultures between wild-type and C/EBPβ−/− rib chondrocytes (Figure 4B). Cyclin B1, B2, and p21 were not significantly altered by the C/EBPβ deficiency, while p16 showed contradictory upregulation. Cyclin D1 and p57 were confirmed to be upregulated and downregulated, respectively, by the loss-of-function of C/EBPβ. However, when the expressions were further compared between primary chondrocytes with retroviral overexpression of C/EBPβ and the control GFP, the cyclin D1 was not downregulated, whereas p57 was upregulated by the C/EBPβ overexpression. These indicate that p57 was the only cell cycle factor whose expression was confirmed to be regulated positively and negatively by the gain- and loss-of-functions of C/EBPβ, respectively. Double immunofluorescence of p57 and BrdU in the

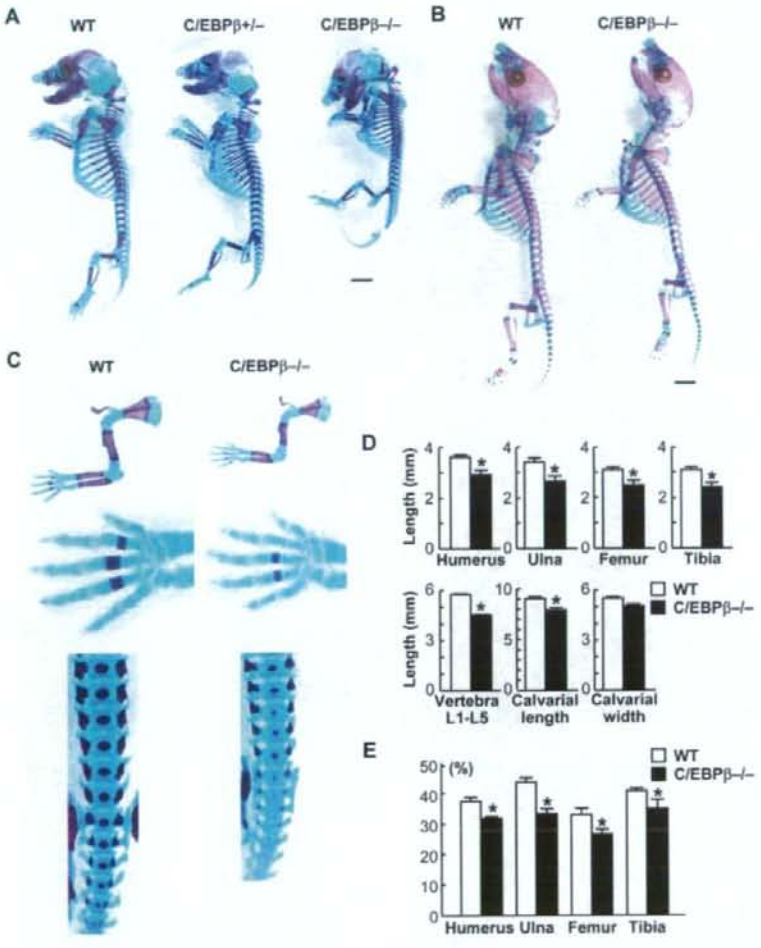

Figure 1. C/EBPβ−/− mice exhibit impaired skeletal growth and endochondral ossification. (A, B) Double stainings with Alizarin red and Alcian blue of the whole skeleton of the wild-type (WT), C/EBPβ+/−, and C/EBPβ−/− littermates at E16.5 (A) and at 3 d after birth (B). Scale bar, 2 mm. (C) Double stainings of the upper limbs, hands, and lumbar spines of the two genotypes. (D) Length of humerus, ulna, femur, tibia, vertebra (1st to 5th lumbar spines), and the calvarial length and width of the WT and C/EBPβ−/− littermates. (E) The percent ratio of Alizarin red-positive mineralized area to total length of the long bones of the two genotypes. Data are expressed as means (bars)±SEM (error bars) of 4 bones per genotype. *P<0.01 vs. WT.
doi:10.1371/journal.pone.0004543.g001

wild-type cartilage revealed that p57 was localized predominantly in late proliferative and pre-hypertrophic chondrocytes which do not exhibit BrdU uptake (Figure 4C). The p57 expression was confirmed to be decreased in the C/EBPβ−/− cartilage.

C/EBPβ transactivates p57 through direct binding to a C/EBP motif

To know the mechanism underlying the induction of p57 expression by C/EBPβ, we analyzed the promoter activity of p57 using human hepatoma HuH-7 cells and ATDC5 cells transfected with a luciferase reporter gene construct containing the 5′-flanking sequences from −1,092 to +226 bp of the p57 promoter (Figure 5A). The transcriptional activity determined by the luciferase-reporter assay was enhanced by co-transfection with C/EBPβ in both cells, indicating the transcriptional induction of p57 by C/EBPβ. Deletion analysis by a series of 5′-deletion constructs identified the responsive element to C/EBPβ as being located between −150 and −130 bp region. The tandem-repeat constructs of this region were confirmed to respond to the C/EBPβ overexpression depending on the repeat number in both cells (Figure 5B). As this region contained a putative C/EBP-binding motif [15], the site-directed mutagenesis was carried out by creating two mutations in the motif. Both of the mutations caused partial but significant suppression of the promoter activity in both cells, indicating that the C/EBP motif is a responsive

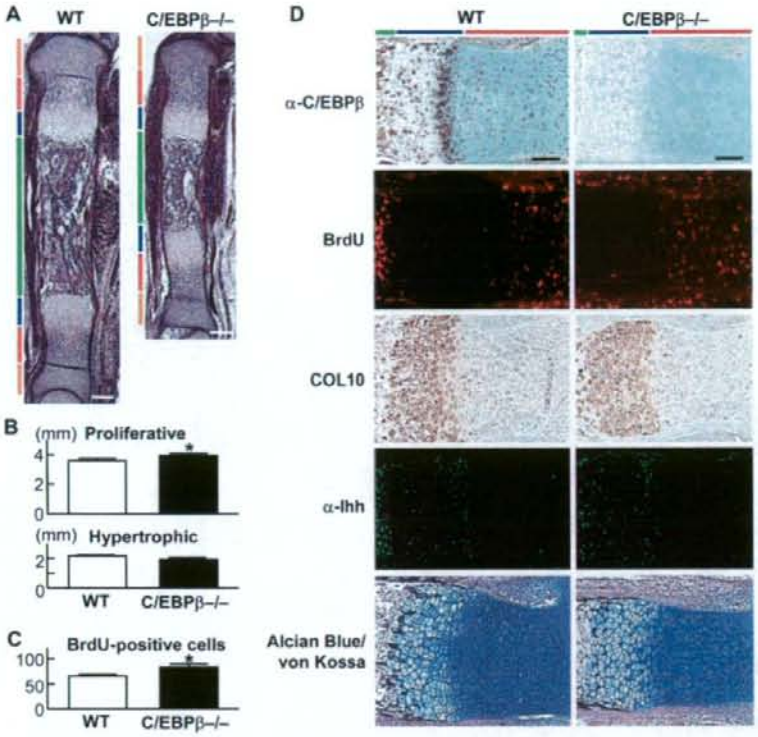

Figure 2. Hypertrophic differentiation of chondrocytes is delayed in the C/EBPβ−/− limb cartilage. (A) HE staining of whole tibias of wild-type (WT) and C/EBPβ−/− littermate embryos (E16.5). Orange, red, blue, and green bars indicate layers of resting zone, proliferative zone, hypertrophic zone, and bone area, respectively. Scale bars, 200 μm. (B) Length of proliferative and hypertrophic zones of the two genotypes. (C) Number of BrdU-positive cells in the proximal tibia of the two genotypes. Data are expressed as means (bars)±SEM (error bars) of 5 mice per genotype. *P<0.05 vs. WT. (D) Immunostaining with an antibody to C/EBPβ (α-C/EBPβ), BrdU labeling, in situ hybridization of type X collagen (COL10), immunostaining with an antibody to Ihh (α-Ihh), and Alcian blue/von Kossa double stainings of the tibial cartilage in two genotypes. Color bars indicate layers as above. Scale bars, 100 μm.
doi:10.1371/journal.pone.0004543.g002

element (Figure 5C). EMSA revealed the specific binding of the nuclear extract from C/EBPβ-overexpressed ATDC5 cells with the oligonucleotide probe containing the identified responsive element above (Figure 5D). The mutagenesis in the C/EBP motif of the probe resulted in a failure to form the complex. Cold competition with excess amounts of an unlabeled wild-type probe, but not the mutated probe, suppressed the complex formation, confirming the specific binding to the C/EBPβ motif. Specificity of C/EBPβ binding was further verified by the antibody supershift. These lines of results demonstrate that C/EBPβ transactivates the p57 promoter, at least in part, through direct binding to a C/EBP motif between the −150 and −130 bp region.

The C/EBPβ-p57 signal induces chondrocyte hypertrophic differentiation

To know the functional interaction between C/EBPβ and p57 during chondrocyte hypertrophic differentiation, we established two small interfering RNA (siRNA) constructs of p57 for the gene silencing. We initially confirmed significant decreases of p57 protein and mRNA levels by stable transfection of the two siRNAs (Figure 5E). The C/EBPβ-induced hypertrophic differentiation of cultured rib chondrocytes determined by ALP staining and COL10 expression was suppressed by the p57 knockdown through the siRNA (Figure 5F), indicating the mediation of p57 in the C/EBPβ induction of hypertrophic differentiation. We confirmed that retroviral overexpression of p57 enhanced the hypertrophy markers in cultured ATDC5 cells (Figure 5G).

C/EBPβ is involved in cartilage destruction during osteoarthritis progression

In addition to the physiological role in skeletal growth in embryos, we finally examined the contribution of C/EBPβ in chondrocytes under pathological conditions. We and others have reported that endochondral ossification including chondrocyte hypertrophy is a crucial step for cartilage destruction during osteoarthritis progression [16–20]. We therefore created an experimental osteoarthritis model that induces instability to the knee joints in 8-week-old wild-type mice [17,21], and found that C/EBPβ was localized at the frontline of cartilage degradation in the central and peripheral areas of the joint cartilage during osteoarthritis progression (Figure 6A). To know the functional involvement of C/EBPβ under the pathological conditions, we

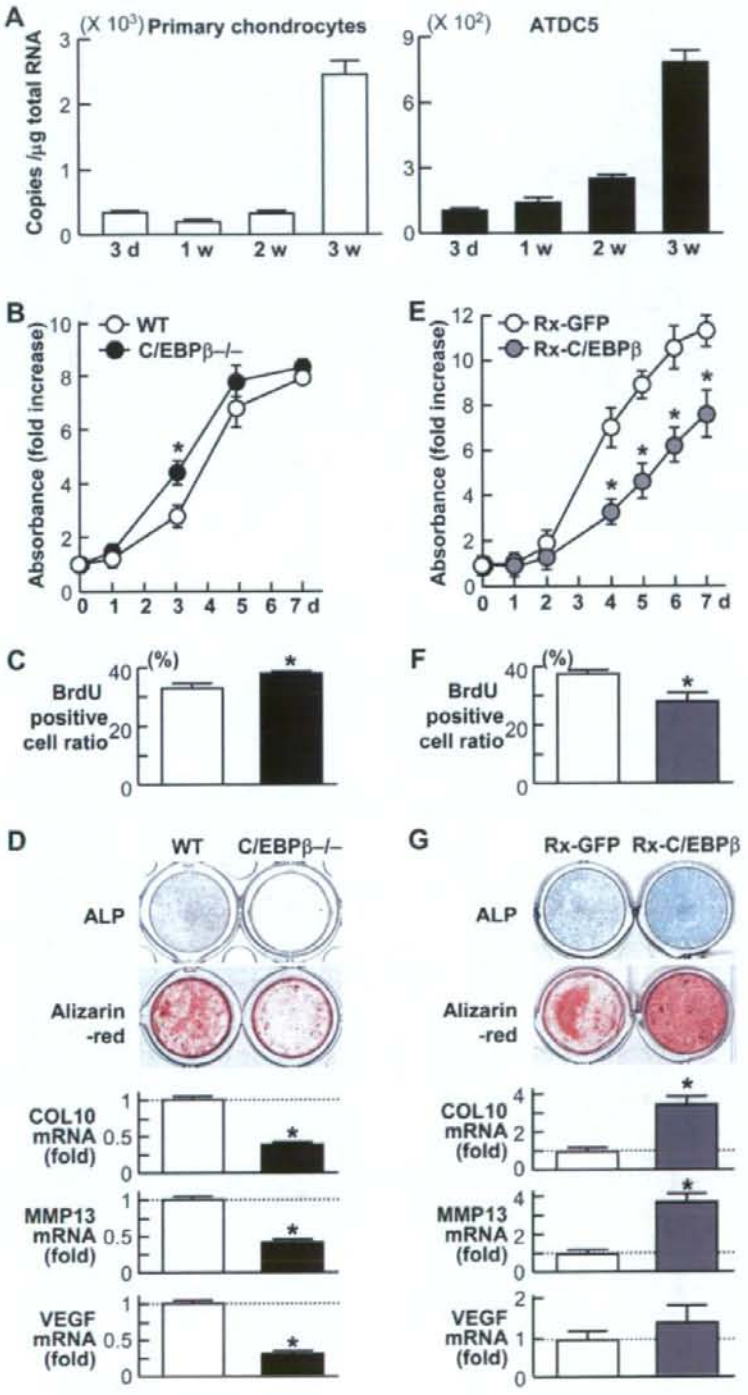
A
(X 10³) Primary chondrocytes
Copies /μg total RNA
3 d
1 w
2 w
3 w
(X 10²) ATDC5
B
WT
C/EBPβ–/–
Absorbance (fold increase)
E
Rx-GFP
Rx-C/EBPβ
C
BrdU positive cell ratio
(%)
F
D
WT
C/EBPβ–/–
ALP
Alizarin -red
COL10 mRNA (fold)
MMP13 mRNA (fold)
VEGF mRNA (fold)
G
Rx-GFP
Rx-C/EBPβ

Figure 3. C/EBPβ inhibits proliferation and promotes hypertrophic differentiation in cultured primary chondrocytes. (A) Time course of C/EBPβ mRNA level determined by real-time RT-PCR analysis during differentiation of primary chondrocytes and ATDC5 cells cultured for 3 weeks with insulin. (B) Growth curves by the XTT assay of primary chondrocytes derived from ribs of wild-type (WT) and C/EBPβ−/− littermates. (C) Ratio of BrdU-positive cells to total cells after 3 d culture of primary chondrocytes derived from WT and C/EBPβ−/− ribs. (D) ALP and Alizarin red stainings, and relative mRNA levels of COL10, MMP13, and VEGF of the primary chondrocytes from the two genotypes determined by real-time RT-PCR analysis at 2 weeks of culture after confluency. (E) Growth curves of primary WT rib chondrocytes with retroviral transfection of C/EBPβ (Rx-C/EBPβ) or the control GFP (Rx-GFP). (F) Ratio of BrdU-positive cells to total cells after 4 d culture of primary WT rib chondrocytes with Rx-C/EBPβ or Rx-GFP. (G) ALP and Alizarin red stainings, and relative mRNA levels of the chondrocyte hypertrophy markers of the rib chondrocytes with Rx-C/EBPβ or Rx-GFP at 2 weeks of culture after confluency. All data are expressed as means (symbols or bars)±SEM (error bars) of 6 wells or dishes per group. *P<0.01 vs. WT or Rx-GFP.
doi:10.1371/journal.pone.0004543.g003

compared the cartilage destruction between C/EBPβ+/− and the wild-type littermates that showed similar phenotypes under physiological conditions (Figure 1A) [9]. C/EBPβ−/− mice were not used in this experiment since their skeleton was originally small, the joint shape was abnormal, and the activity was low, so that mechanical stress caused by the joint instability was not assumed to be comparable to that of wild-type mice. The cartilage destruction as well as COL10 expression was suppressed in C/EBPβ+/− mice, remaining a substantial undegraded matrix even 8 to 12 weeks after the surgery (Figure 6B). Quantification using the OARSI grading system [22] confirmed significant prevention of cartilage destruction by the C/EBPβ haploinsufficiency (Figure 6C).

Discussion

The present study for the first time demonstrated that the transcription factor C/EBPβ is essential for physiological skeletal growth and endochondral ossification by analyses of the deficient mice. This function was dependent on the promotion of transition from proliferation to hypertrophic differentiation of chondrocytes through the cell cycle control. Our further screening of cell cycle factors identified the cyclin-dependent kinase inhibitor p57 as the transcriptional target, and detected a responsive element of C/EBPβ in the promoter. We finally showed the functional mediation of p57 in the C/EBPβ action, and confirmed the importance of the C/EBPβ-p57 signal in the chondrocyte hypertrophy during skeletal growth and osteoarthritis progression.

Growth retardation of C/EBPβ−/− mice was seen during embryogenesis only and disappeared as the animals grew up after birth under physiological conditions (Figure 1A & B). This may possibly be due to compensatory mechanisms by other C/EBP family members which are known to control cellular differentiation in several lineages [23–26]. Regarding the mesenchymal cell lineage, C/EBPδ has been reported to show similar and compensatory actions for adipogenic and osteogenic differentiation [11,27–31]. Since the involvement of C/EBPδ in chondrogenic differentiation from the mesenchymal precursors remains unknown, we initially examined the expression by immunohistochemistry in the limb cartilage (E16.5) (Figure S1A). It was expressed predominantly in late proliferative and pre-hypertrophic chondrocytes, similarly to the C/EBPβ expression, and this was not altered in the C/EBPβ−/− cartilage. In addition, retroviral overexpression of C/EBPδ enhanced hypertrophic differentiation determined by COL10 and MMP13 mRNA levels in cultured ATDC5 cells (Figure S1B). Furthermore, the p57 promoter activity was enhanced by the C/EBPδ overexpression, although the effect was somewhat weaker than that by C/EBPβ (Figure S1C). Although we could not detect the distinct regulation of C/EBPβ and C/EBPδ expressions in the limb chondrocytes before and after birth, their actions on chondrocyte hypertrophy might be compensatory, especially postnatally. We are now investigating the role of C/EBPδ in the skeletal growth using the knockout mice as well as the double knockout mice of C/EBPβ and C/EBPδ.

The runt family transcription factor member Runx2 [1,32,33], parathyroid hormone/parathyroid hormone-related protein (PTH/PTHrP) [1,34], and cyclic GMP-dependent protein kinase II (cGKII) [35,36] are known as representative regulators of chondrocyte hypertrophy, and interestingly, C/EBPβ has been reported to be associated with these representative regulators. C/EBPβ acts as a co-activator of Runx2 [6,37]. Generally, the complex of the members of the C/EBP and Runx families is known to interact in the activation of lineage-specific promoters during differentiation of osteoblasts, adipocytes, and granulocytes [6]. Unlike Runx2−/− mice that exhibit a complete lack of bone [32], C/EBPβ−/− mice showed almost normal bone, raising the possibility of functional redundancy with other isoforms such as C/EBPα or C/EBPδ in osteoblast differentiation. Contrarily, both Runx2−/− and C/EBPβ−/− mice showed impairment of chondrocyte hypertrophy during cartilage development and growth [32,33], implicating a specific interaction between C/EBPβ and Runx2 in cartilage. In the present study, the site-directed mutagenesis in the C/EBP motif of the p57 promoter caused significant but incomplete suppression of the promoter activity induced by the C/EBPβ overexpression (Figure 5C). Actually, there is a putative Runx motif which lies close to this C/EBP motif in this region. C/EBPβ might therefore stimulate the promoter activity at the Runx motif as a co-activator of Runx2, even after the innate binding was blocked, although our luciferase assay and EMSA so far have failed to find evidence of this.

Contrarily to Runx2, PTH/PTHrP keeps chondrocytes proliferating and inhibits their hypertrophic differentiation [1,34]. The PTH/PTHrP action via the adenyl cyclase signal in chondrocytes is reported to be dependent on the suppression of p57 expression [38], implicating a possible mediation of C/EBPβ in this pathway. However, our present study showed that neither PTH nor the adenyl cyclase activator forskolin affected the C/EBPβ protein level in cultured ATDC5 cells or the activity of the p57 promoter (−150 to +226 bp) with or without induction by C/EBPβ (Figure S2). Although C/EBPβ is therefore unlikely to mediate the p57 suppression by PTH/PTHrP directly, its possible involvement as a co-activator of Runx2 again cannot be denied here, since the PTH/PTHrP action is also at least partly dependent on the Runx2 suppression in chondrocytes [39].

cGKII is a serine/threonine kinase lying downstream of the C-type natriuretic peptide pathway which is essential for skeletal growth [40]. We and others have reported that the deficiency of cGKII in mice and rats caused dwarfism due to impaired hypertrophic differentiation of chondrocytes [35,41], similarly to the present C/EBPβ−/− mice. Interestingly, a previous study showed that cGKII activated C/EBPβ through phosphorylation of glycogen synthase kinase-3β (GSK-3β) in osteosarcoma cells [42], and our recent study showed that cGKII induced chondrocyte hypertrophic differentiation through the GSK-3β phosphorylation [36]. These suggest a possible mediation of the present C/EBPβ-

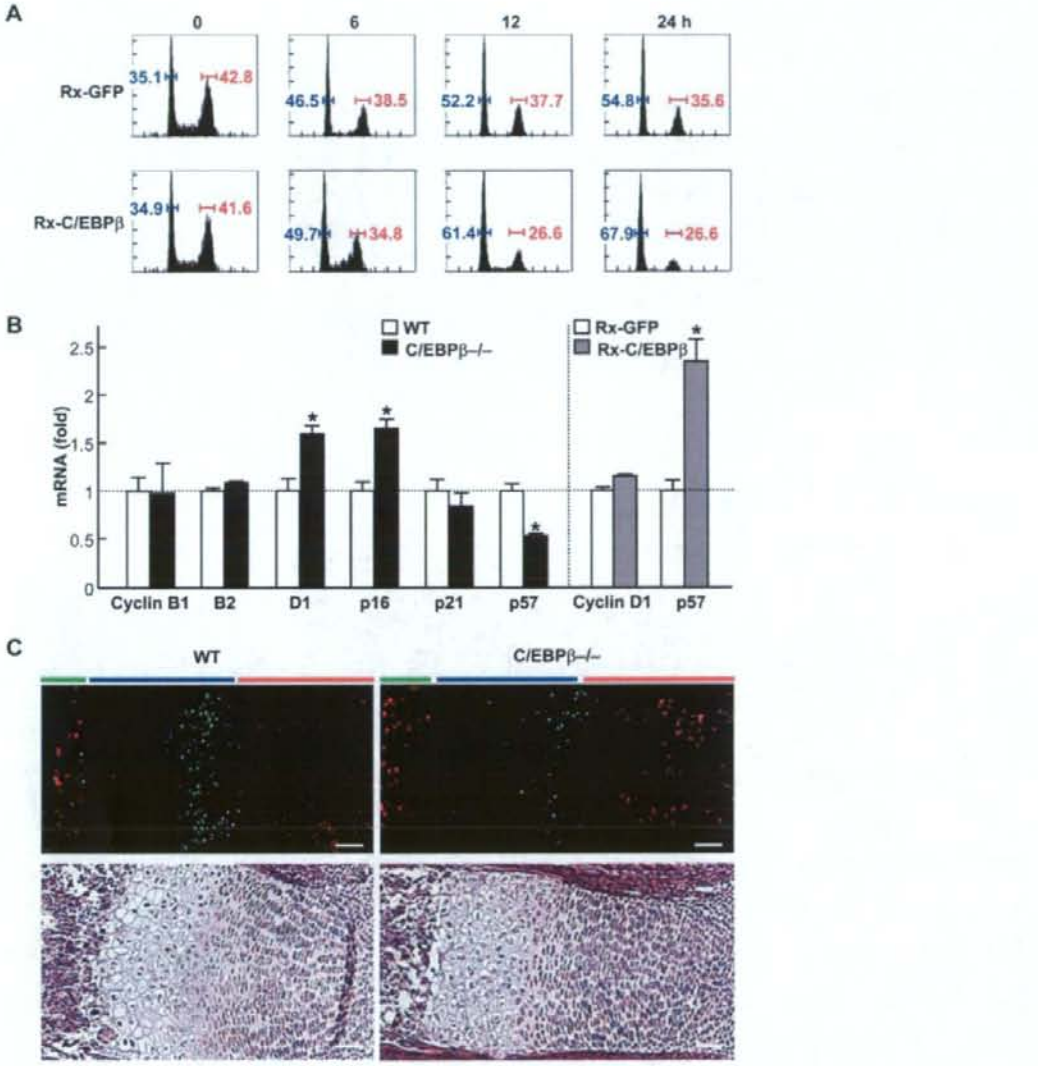

Figure 4. C/EBPβ affects cell cycle factors. (A) Time course of DNA histograms by a flow cytometric analysis of C3H10T1/2 cells with retroviral transfection of C/EBPβ (Rx-C/EBPβ) or the control GFP (Rx-GFP) after synchronization at the G2/M phase by nocodazole treatment. The horizontal and vertical axes represent the DNA content and relative frequency, respectively. The blue and red bars indicate the rates of cells in G0/G1 and G2/M phases, respectively. (B) Effects of loss- and gain-of-functions of C/EBPβ on relative mRNA levels of cell cycle factors that were identified as possible transcriptional targets of C/EBPβ by a microarray analysis (Table S1). The levels were compared by real-time RT-PCR analysis in the cultures between wild-type (WT) and C/EBPβ−/− rib chondrocytes (left), and between WT rib chondrocytes with Rx-C/EBPβ and Rx-GFP (right). Data are expressed as means (bars)±SEM (error bars) of 6 samples per group. (C) Double immunofluorescence of p57 (green) and BrdU (red) in the proximal cartilage of tibias of the two genotype embryos (E16.5) and the HE staining (bottom) as a reference. Red, blue, and green bars indicate layers of proliferative zone, hypertrophic zone, and bone area, respectively. Scale bars, 50 μm.
doi:10.1371/journal.pone.0004543.g004

p57 signal in the cGKII-GSK-3β action. However, neither cGKII nor GSK-3β overexpression altered at least the activity of the p57 promoter (−150 to +226 bp) with or without induction by C/EBPβ (Figure S3). Moreover, there is a marked difference in the limb cartilage phenotype between cGKII−/− and C/EBPβ−/− mice. Unlike the cGKII−/− cartilage characterized by appearance of a wide abnormal intermediate layer between the proliferative and hypertrophic zones [35,41], the C/EBPβ−/−

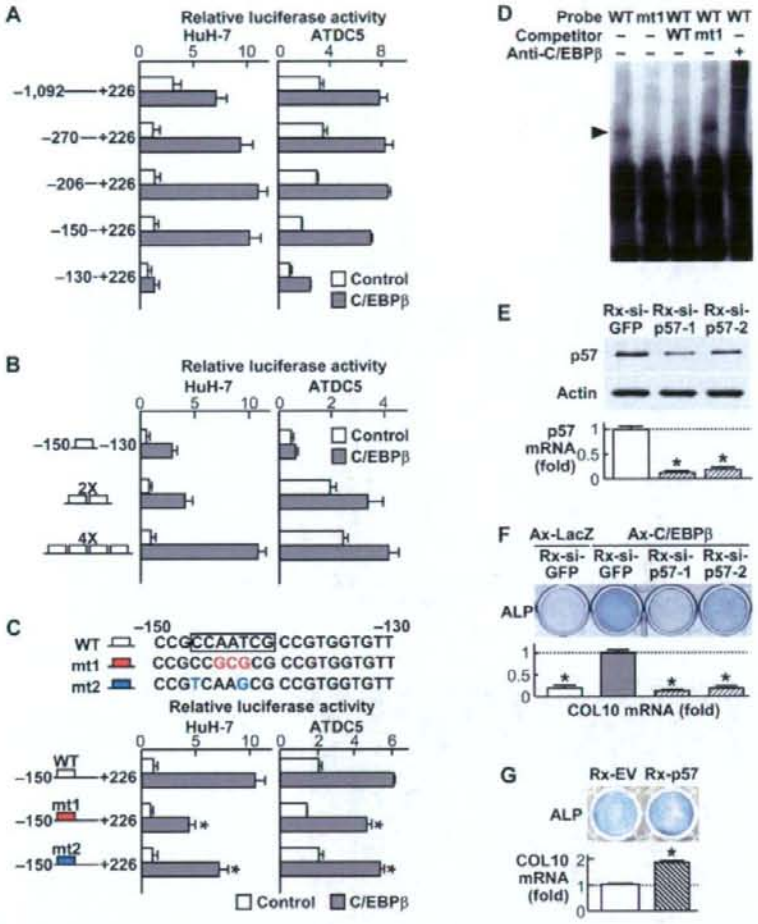

Figure 5. C/EBPβ transactivates p57 through binding to a C/EBP motif and the C/EBPβ-p57 signal induces chondrocyte hypertrophic differentiation. (A) Deletion analysis using luciferase-reporter constructs containing the 5′-flanking sequences from −1,092 to +226 bp of the p57 promoter and a series of deletion fragments in HuH-7 and ATDC5 cells transfected with C/EBPβ or the control GFP. (B) Dose-response analysis of the tandem repeats of the identified responsive element (−150/−130) by the luciferase-reporter assay in the HuH-7 and ATDC5 cells. (C) Site-directed mutagenesis analysis by two mutations (mt1 and mt2) in the C/EBPβ motif (−147/−141) as compared to the wild-type (WT) construct by the luciferase-reporter assay in HuH-7 and ATDC5 cells. *P<0.01 vs. WT-C/EBPβ. (D) EMSA for specific binding of the nuclear extract from C/EBPβ-transfected ATDC5 cells with the oligonucleotide probe (−160/−120) containing the WT or mt1 C/EBPβ motif. The arrowhead indicates the complex. Cold competition with 50-fold excess of unlabeled WT or mt1 probe, and supershift by an antibody to C/EBPβ of the complex are also presented. (E) The protein and mRNA levels of p57 determined by immunoblotting and real-time RT-PCR, respectively, by the p57 siRNA. Stable lines of C3H10T1/2 cells retrovirally transfected with two kinds of siRNA of p57 (Rx-si-p57-1 and Rx-si-p57-2) or the control GFP siRNA (Rx-si-GFP) were established. *P<0.01 vs. Rx-si-GFP. (F) Effects of the p57 siRNA above on the C/EBPβ-induced hypertrophic differentiation of chondrocytes. Primary rib chondrocytes were transfected with Rx-si-p57-1, Rx-si-p57-2, or Rx-si-GFP, and further adenovirally co-transfected with C/EBPβ or the control LacZ (Ax-C/EBPβ or Ax-LacZ). Hypertrophic differentiation was determined by ALP staining and relative COL10 mRNA level by real-time RT-PCR analysis at 2 weeks of culture after confluency. *P<0.01 vs. Ax-C/EBPβ with Rx-si-GFP. (G) Hypertrophic differentiation of ATDC5 cells stably transfected with the retrovirus expressing p57 (Rx-p57) or the empty vector (Rx-EV) cultured for 3 weeks with insulin and further for 2 d with inorganic phosphate. *P<0.01 vs. Rx-EV. All graphs are expressed as means (bars)±SEM (error bars) for 6 wells/group.
doi:10.1371/journal.pone.0004543.g005

cartilage only exhibited an elongated proliferative zone and delayed chondrocyte hypertrophy (Figure 2D). Hence, the cell cycle arrest in chondrocytes caused by C/EBPβ appears to immediately link to the start of the differentiation. The discrepancy may be due to the diversity of signaling pathway(s) lying downstream of cGKII and upstream of C/EBPβ. We previously reported that cGKII phosphorylated Sox9, an inhibitor of chondrocyte hypertrophy, and suppressed its nuclear entry [35]. Besides Sox9 and GSK-3β, vasodilator-stimulated phosphoprotein and cysteine- and glycine-rich protein 2 are putative phosphor-

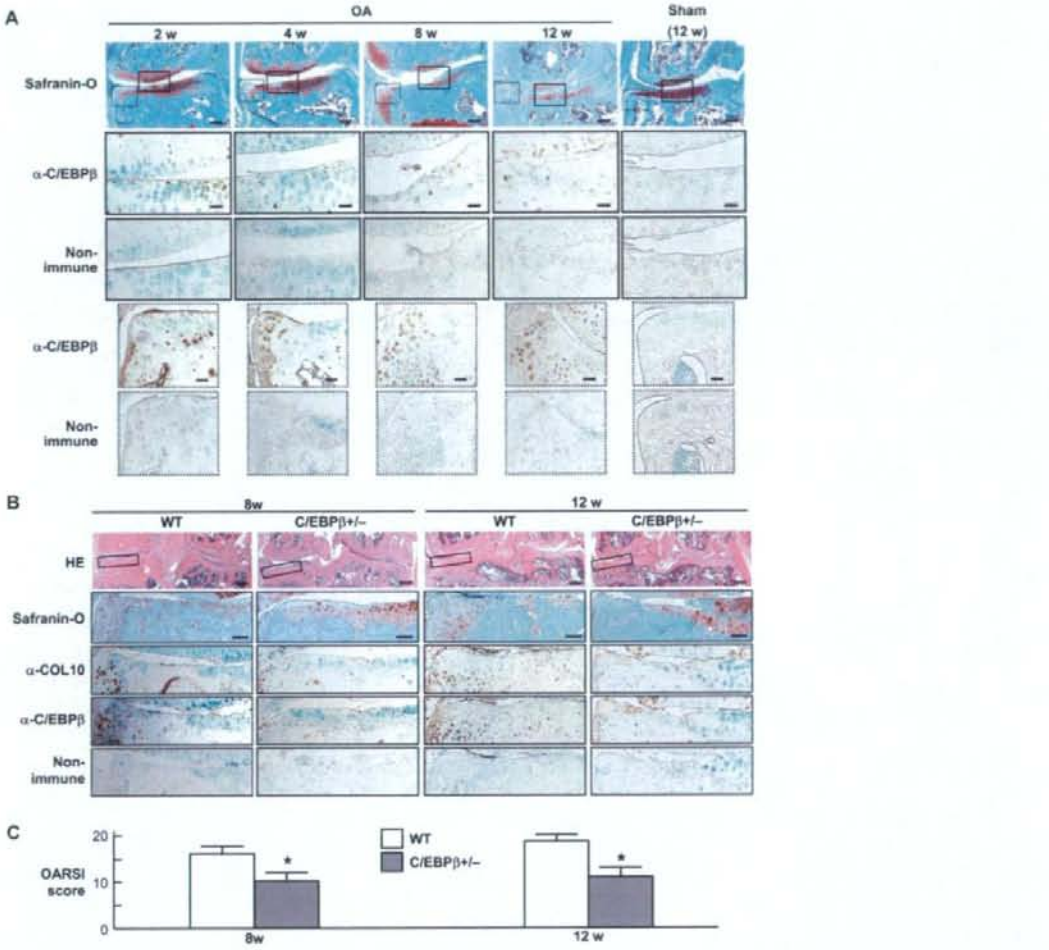

Figure 6. C/EBPβ is involved in cartilage destruction during osteoarthritis progression. (A) Time course of joint cartilage destruction and C/EBPβ expression in the medial portion of cartilage after creating an experimental osteoarthritis model that induces instability to the knee joints of 8-week-old wild-type mice. Safranin-O staining and immunohistochemical staining with an antibody to C/EBPβ (α-C/EBPβ) or the non-immune control IgG were performed at the indicated weeks after surgery. A sham operation was performed using the same approach, and assessed after 12 weeks. Boxed areas with solid and dotted lines in the top row indicate the regions of the other rows. Scale bars, 100 μm (top) and 400 μm (others). (B) HE and Safranin-O stainings, and immunohistochemical stainings with α-C/EBPβ and α-COL10 or the non-immune IgG in the tibial cartilage of wild-type (WT) and C/EBPβ+/− littermates 8 weeks and 12 weeks after the surgery. Boxed areas in the top row indicate the regions of the other rows. Scale bars, 200 μm (top), 400 μm (others). (C) Cartilage destruction according to the OARSI grading system. Data are expressed as means (bars) ± SEM (error bars) for 5 mice per genotype at 8 and 12 weeks. *$P<0.05$ vs. WT
doi:10.1371/journal.pone.0004543.g006

ylation targets of cGKII in other types of cells [43]. In addition to the abovementioned GSK-3β, C/EBPβ is also targeted by multiple protein kinases including protein kinase A, calmodulin-dependent protein kinase, Erk-1/2, ribosomal protein S6 kinase, and CDK2 [44].

The skeletal abnormalities of C/EBPβ−/− mice were much milder than those of the p57−/− mice which were perinatally lethal due to various defects analogous to Beckwith-Weidemann syndrome in children, including cleft palate and body wall dysplasia besides severe dwarfism [38,45–47]. This may be because p57 is more crucial for chondrocyte hypertrophic differentiation than C/EBPβ whose function could be substituted by several upstream signals of p57. In fact, the C/EBPβ deficiency did not abrogate, but partially suppressed the p57 expression in chondrocytes (Figure 4B, C), while the knockdown of p57 strongly suppressed the C/EBPβ-induced hypertrophic differentiation of chondrocytes (Figure 5F). Among other cell cycle factors, mice lacking the Rb-related pocket proteins p107 and p130 show skeletal phenotype very similar to that of the p57−/− mice [48], indicating that these proteins are likely to be major downstream

targets of the cyclin-CDK complexes that are inhibited by p57 in chondrocytes. More interestingly, the Cip/Kip family proteins have recently been reported to regulate pathways distinct from that of cell cycle control [14]. Since p57 supports skeletal myoblast differentiation by inhibiting phosphorylation of the key transcription factor MyoD [49], this factor might also induce chondrocyte hypertrophic differentiation by regulating crucial transcription factors like Runx2 or Sox9. This may also explain the direct linkage from the cell cycle arrest to cell differentiation by the C/EBPβ-p57 signaling, unlike the cGKII signal, as mentioned above.

We conclude that C/EBPβ directly transactivates p57 to promote transition from proliferation to hypertrophic differentiation of chondrocytes during endochondral ossification. Besides the anabolic function for physiological skeletal growth, the C/EBPβ haploinsufficiency in adult mice caused resistance to cartilage destruction during osteoarthritis progression in knee joints (Figure 6). Furthermore, C/EBPβ has been reported to be induced by proinflammatory cytokines interleukin-1 and tumor necrosis factor-α, and to mediate the decrease of articular cartilage matrix by suppressing the promoter activity of cartilage characteristic genes like cartilage-derived retinoic acid-sensitive protein and type II collagen [50–52]. The cytokine-induced C/EBPβ also enhances the promoter activity of prostaglandin synthetic enzymes like cyclooxygenase-2 and phospholipase A2 [53,54] and proteinases like aggrecanase-1 and matrix metalloproteinase-1 [55,56] in chondrocytes. These lines of evidence indicate that the C/EBPβ-p57 signal could be a therapeutic target of inflammatory and degenerative joint disorders as well as skeletal growth retardation.

Materials and Methods

Ethics statement

All experiments were performed according to the protocol approved by the Animal Care and Use Committee of the University of Tokyo.

Animals

C/EBPβ deficient mice, kindly provided by Dr. Shizuo Akira (University of Osaka), were maintained in a C57BL/6 background. In each experiment, we compared C/EBPβ−/− or C/EBPβ+/− mice with the wild-type littermates.

Histological analysis

The whole skeletons of WT and C/EBPβ−/− littermate embryos (E16.5) were fixed in 99.5% ethanol, transferred to acetone, and stained in a solution containing Alizarin red S and Alcian blue 8GX (Sigma). For histological analysis, tibial limbs were fixed in 4% paraformaldehyde (PFA) buffered with PBS and sectioned in 5-μm slices. Hematoxylin-eosin (HE) stainings were performed according to standard protocols. Alcian blue/von Kossa double stainings were performed with 1% Alcian blue 8GX in 3% acetate and with 5% silver nitrate. For immunohistochemistry, the sections were incubated with antibodies to C/EBPβ (C-19), p57 (C-20), Ihh (C-15), and C/EBPδ (M-17) (Santa Cruz Biotechnology Inc.) diluted 1:500 in blocking reagent. The localization of C/EBPβ was detected with HRP-conjugated secondary antibody (Promega). For fluorescent visualization, a secondary antibody conjugated with Alexa Fluor 488 (Invitrogen) was used. The p57 detection was performed using a CSA II, Biotin-Free Catalyzed Amplification System (DAKO). In situ hybridization was performed, as we reported previously [21]. Briefly, hybridization with complementary digoxigenin (DIG)-labeled for mouse type X collagen was performed in a humidified chamber for 16 h at 52°C. For the detection of DIG-labeled probes, slides were incubated with HRP-conjugated anti-DIG rabbit polyclonal antibody (Dakopatts). The sections were immersed in a diaminobenzidine solution to visualize immunoreactivity. For BrdU labeling, we injected BrdU (Sigma) intraperitoneally to pregnant mice prior to sacrifice, and the sections were stained using a BrdU Immunohistochemistry System (Calbiochem) and Alexa Fluor 568 (Molecular Probes).

Cell cultures

Primary chondrocytes were isolated from the ribs of mouse embryos as previously described [57]. The primary chondrocytes, HuH-7 cells and C3H10T1/2 cells were cultured in DMEM with 10% FBS. ATDC5 cells were maintained in DMEM/F12 with 5% FBS. To induce hypertrophic differentiation, the ATDC5 cells were cultured for 3 weeks with insulin.

Plasmids and viral vectors

C/EBPβ and p57 cDNA were cloned into pMx vectors, and retroviral vectors were generated using plat-E cells [58]. The siRNA sequence was designed for the mouse p57 gene (NM_009876.3: nucleotides 925–946 and 307–328) and GFP as previously described [59] and ligated into piGENEmU6 vector (iGENE Therapeutics). The siRNA sequence combined with the promoter was then inserted into a retroviral pMx vector. The adenovirus C/EBPβ and LacZ expression vector were synthesized using an Adeno-X expression system (Clontech). Two weeks after transfection, the cells were harvested and used for subsequent assays. cDNA of cGKII and GSK-3β was ligated into pCMV-HA (Invitrogen).

Cell proliferation assay

Primary chondrocytes were inoculated at 10^3 cells per well in a 96-well plate. The proliferation of cells was examined, using an XTT Assay Kit (Roche) at the indicated time point. The absorbance of the product was quantified using a MTP-300 microplate reader (Corona Electric). For BrdU detection analysis, we labeled the chondrocytes with 10 μM BrdU (Sigma) for 18 h and the cells were stained using a BrdU Immunohistochemistry System (Calbiochem).

Chondrocyte differentiation assay

Primary chondrocytes were cultured for two weeks after confluency, and the total RNA was extracted to assess the COL10, MMP13, and VEGF mRNA levels. For the ALP staining, cells were stained with a solution containing 0.01% Naphthol AS-MX phosphate disodium salt (Sigma), 1% N, N-dimethyl-formamide (Wako), and 0.06% fast blue BB (Sigma). For the Alizarin red S staining, cells were stained with 2% Alizarin red S solution (Sigma).

Flow cytometric analysis

C3H10T1/2 cells with retroviral transfection with C/EBPβ or GFP were incubated for 18 h in the presence of 0.2 μM nocodazole for synchronization at the G2/M phase. Then, cells were suspended in citrate buffer and stained with propidium iodide. DNA content was analyzed with EPICS XL and XL EXPO32 instruments (Beckman).

Real-time RT-PCR

The total RNA was extracted using an ISOGEN Kit (Wako) and an RNeasy Mini Kit (QIAGEN). One μg of RNA was reverse-transcribed with a Takara RNA PCR Kit (AMV) ver.2.1 (Takara) to generate single-stranded cDNA. PCR was performed with an ABI Prism 7000 Sequence Detection System (Applied Biosystems). All reactions were run in triplicate. Primer sequence information is available upon request.

Luciferase assay

The human p57 promoter regions were cloned into the pGL4.10 vector (Promega). Other deletion constructs were created by the PCR technique. Tandem-repeat constructs were created by ligating the double strand oligonucleotides from −150 to −130 bp into pGL4.10 vector. Transfection in HuH-7 and ATDC5 cells was performed in quadruplicate using Fugene (Roche). For PTH or forskolin stimulation, cells were cultured with PTH (10 nM) or forskolin (10 nM) at the time of transfection. The luciferase assay was performed with a PicaGene Dual SeaPansy Luminescence Kit (Toyo Ink) and GloMax™ 96 Microplate Luminometer (Promega).

Electrophoretic Mobility Shift Assay (EMSA)

Nuclear extracts were prepared from ATDC5 cells adenovirally transfected with C/EBPβ. Oligonucleotide probes of the −160 to −120 bp region sequence in the p57 promoter were labeled with digoxigenin by using a DIG gel shift kit (Roche). For competition analyses, 50-fold excess of unlabeled competitor probe was included in the binding reaction. For the supershift experiments, 1 μL of an antibody to C/EBPβ (Santa Cruz Biotechnology Inc.) was added.

Microarray analysis

Total RNA was isolated from C3H10T1/2 cells with retroviral introduction of C/EBPβ or the empty vector after 1 week of culture. The microarray experiment was performed using the Gene Chip Mouse Genome 430 2.0 Array (Affymetrix), scanned by GeneChip Scanner 3000, and analyzed using GCOS ver 1.4 software.

Immunoblotting

ATDC5 cells were cultured with PTH (10 nM) or forskolin (10 nM) for 0 to 30 min, and then their cytoplasmic and nuclear proteins were extracted with an NE-PER (Pierce Chemical). For immunoblot analysis, lysates were fractionated by SDS-PAGE and transferred onto nitrocellulose membranes (BIO-RAD). The membranes were incubated with an antibody to C/EBPβ (Santa Cruz), or an antibody to actin (Sigma). Immunoreactive bands were visualized with ECL Plus (Amersham Biosciences).

Osteoarthritis experiment

The surgical procedure to create an osteoarthritis experimental model was performed on 8-week-old male mice, as we have reported previously [17,20,21]. At the indicated time points after surgery, the mice were killed, and the entire knee joints were dissected and fixed for 24 h at 4°C in 4% PFA. The specimens were decalcified for 2 weeks with 10% EDTA (pH 7.4) at 4°C and sectioned in 5-μm slices. Sections were stained with Safranin O–fast green. Destruction of cartilage was quantified according to the OARSI grading system [22]. For immunohistochemistry, the sections were incubated with antibodies to C/EBPβ (Santa Cruz), COL10 (LSL) or the nonimmune rabbit IgG as the negative control diluted 1:500 in blocking reagent, and the localization was detected with HRP-conjugated secondary antibody (Promega).

Statistical analysis

Means of groups were compared by ANOVA, and significance of differences was determined by post-hoc testing using Bonferroni's method.

Supporting Information

Table S1 Microarray analysis shows the changes in expression of cell cycle factors by C/EBPβ overexpression. Ratios of mRNA levels in C3H10T1/2 cells with retroviral introduction of C/EBPβ in comparison with the control empty vector were determined by Gene Chip Mouse Genome 430 2.0 Array (Affymetrix). All results of the microarray analysis are provided at ArrayExpress (accession number: E-MEXP-1984).
Found at: doi:10.1371/journal.pone.0004543.s001 (0.02 MB PDF)

Figure S1 C/EBPδ shows similar expression and function in chondrocytes to those of C/EBPβ. (A) Immunostaining with an antibody to C/EBPδ in the tibial cartilage of wild-type (WT) and C/EBPβ−/− littermates (E16.5). Red, blue, and green bars indicate layers of proliferative zone, hypertrophic zone, and bone area, respectively. Scale bars, 100 mm. (B) Relative mRNA levels of COL10, MMP13, and VEGF of ATDC5 cells with retroviral transfection of C/EBPδ or the control GFP determined by real-time RT-PCR at 2 weeks of culture after confluency. (C) The p57 promoter activity in ATDC5 cells transfected with luciferase-reporter construct containing the 5′-flanking sequences from −150 to +226 bp of the p57 promoter with effector plasmid expressing C/EBPδ, C/EBPβ, or the control GFP. All data are expressed as means (symbols or bars)±SEM (error bars) of 6 wells per group. *P<0.01 vs. GFP.
Found at: doi:10.1371/journal.pone.0004543.s002 (0.68 MB PDF)

Figure S2 PTH and forskolin have no effects on C/EBPβ protein level and p57 promoter activity. (A) Time course of C/EBPβ protein level in cultured ATDC5 cells. After the indicated time of treatment with PTH (10 nM) and forskolin (10 nM), the C/EBPβ protein levels in the cytoplasmic fraction (C) and nuclear fraction (N) were determined by immunoblotting with an antibody to C/EBPβ or actin as the loading control. (B) Effects of PTH, forskolin or the control on HuH-7 cells transfected with luciferase-reporter construct containing the 5′-flanking fragment (−150 to +226 bp) of the p57 promoter with effector plasmid expressing C/EBPβ or GFP as the control. The promoter activity was determined by the luciferase assay after 2 d of treatment.
Found at: doi:10.1371/journal.pone.0004543.s003 (0.07 MB PDF)

Figure S3 Effects of cGKII and GSK-3β overexpression on p57 promoter activity. The promoter activity was determined by the luciferase assay in HuH-7 cells transfected with luciferase-reporter construct containing the 5′-flanking fragment (−150 to +226 bp) of the p57 promoter with effector plasmid expressing C/EBPβ or GFP as the control.
Found at: doi:10.1371/journal.pone.0004543.s004 (0.02 MB PDF)

Author Contributions

Conceived and designed the experiments: MH FK TI KN UiC HK. Performed the experiments: MH FK AF SO TO. Analyzed the data: MH FK AF. Contributed reagents/materials/analysis tools: SO NK TO YK TS FY TI UiC. Wrote the paper: MH NK HK.

References

1. Kronenberg HM (2003) Developmental regulation of the growth plate. Nature 423: 332–336.
2. Hunziker EB (1994) Mechanism of longitudinal bone growth and its regulation by growth plate chondrocytes. Microsc Res Tech 28: 505–519.

3. Wilsman NJ, Farnum CE, Leiferman EM, Fry M, Barreto C (1996) Differential growth by growth plates as a function of multiple parameters of chondrocytic kinetics. J Orthop Res 14: 927–936.
4. Descombes P, Chojkier M, Lichtsteiner S, Falvey E, Schibler U (1990) LAP, a novel member of the C/EBP gene family, encodes a liver-enriched transcriptional activator protein. Genes Dev 4: 1541–1551.
5. Landschulz WH, Johnson PF, Adashi EY, Graves BJ, McKnight SL (1988) Isolation of a recombinant copy of the gene encoding C/EBP. Genes Dev 2: 786–800.
6. Nerlov C (2007) The C/EBP family of transcription factors: a paradigm for interaction between gene expression and proliferation control. Trends Cell Biol 17: 318–324.
7. Johnson PF (2005) Molecular stop signs: regulation of cell-cycle arrest by C/EBP transcription factors. J Cell Sci 118: 2545–2555.
8. Wu Z, Xie Y, Bucher NL, Farmer SR (1995) Conditional ectopic expression of C/EBP beta in NIH-3T3 cells induces PPAR gamma and stimulates adipogenesis. Genes Dev 9: 2350–2363.
9. Screpanti I, Romani L, Musiani P, Modesti A, Fattori E, et al. (1995) Lymphoproliferative disorder and imbalanced T-helper response in C/EBP beta-deficient mice. EMBO J 14: 1932–1941.
10. Tanaka T, Akira S, Yoshida K, Umemoto M, Yoneda Y, et al. (1995) Targeted disruption of the NF-IL6 gene discloses its essential role in bacteria killing and tumor cytotoxicity by macrophages. Cell 80: 353–361.
11. Tanaka T, Yoshida N, Kishimoto T, Akira S (1997) Defective adipocyte differentiation in mice lacking the C/EBPbeta and/or C/EBPdelta gene. EMBO J 16: 7432–7443.
12. LuValle P, Beier F (2000) Cell cycle control in growth plate chondrocytes. Front Biosci 5: D493–503.
13. Moro T, Ogasawara T, Chikuda H, Ikeda T, Ogata N, et al. (2005) Inhibition of Cdk6 expression through p38 MAP kinase is involved in differentiation of mouse prechondrocyte ATDC5. J Cell Physiol 204: 927–933.
14. Besson A, Dowdy SF, Roberts JM (2008) CDK inhibitors: cell cycle regulators and beyond. Dev Cell 14: 159–169.
15. Meergans T, Albig W, Doenecke D (1998) Conserved sequence elements in human main type-H1 histone gene promoters: their role in H1 gene expression. Eur J Biochem 256: 436–446.
16. Drissi H, Zuscik M, Rosier R, O'Keefe R (2005) Transcriptional regulation of chondrocyte maturation: potential involvement of transcription factors in OA pathogenesis. Mol Aspects Med 26: 169–179.
17. Kamekura S, Kawasaki Y, Hoshi K, Shimoaka T, Chikuda H, et al. (2006) Contribution of runt-related transcription factor 2 to the pathogenesis of osteoarthritis in mice after induction of knee joint instability. Arthritis Rheum 54: 2462–2470.
18. Kawaguchi H (2008) Endochondral ossification signals in cartilage degradation during osteoarthritis progression in experimental mouse models. Mol Cells 25: 1–6.
19. Kuhn K, D'Lima DD, Hashimoto S, Lotz M (2004) Cell death in cartilage. Osteoarthritis Cartilage 12: 1–16.
20. Yamada T, Kawano H, Koshizuka Y, Fukuda T, Yoshimura K, et al. (2006) Carminerin contributes to chondrocyte calcification during endochondral ossification. Nat Med 12: 665–670.
21. Kamekura S, Hoshi K, Shimoaka T, Chung U, Chikuda H, et al. (2005) Osteoarthritis development in novel experimental mouse models induced by knee joint instability. Osteoarthritis Cartilage 13: 632–641.
22. Pritzker KP, Gay S, Jimenez SA, Ostergaard K, Pelletier JP, et al. (2006) Osteoarthritis cartilage histopathology: grading and staging. Osteoarthritis Cartilage 14: 13–29.
23. Darlington GJ (1999) Molecular mechanisms of liver development and differentiation. Curr Opin Cell Biol 11: 678–682.
24. Darlington GJ, Ross SE, MacDougald OA (1998) The role of C/EBP genes in adipocyte differentiation. J Biol Chem 273: 30057–30060.
25. Radomska HS, Huettner CS, Zhang P, Cheng T, Scadden DT, et al. (1998) CCAAT/enhancer binding protein alpha is a regulatory switch sufficient for induction of granulocytic development from bipotential myeloid progenitors. Mol Cell Biol 18: 4301–4314.
26. Zhang DE, Hetherington CJ, Meyers S, Rhoades KL, Larson CJ, et al. (1996) CCAAT enhancer-binding protein (C/EBP) and AML1 (CBF alpha2) synergistically activate the macrophage colony-stimulating factor receptor promoter. Mol Cell Biol 16: 1231–1240.
27. Cao Z, Umek RM, McKnight SL (1991) Regulated expression of three C/EBP isoforms during adipose conversion of 3T3-L1 cells. Genes Dev 5: 1538–1552.
28. Gutierrez S, Javed A, Tennant DK, van Rees M, Montecino M, et al. (2002) CCAAT/enhancer-binding proteins (C/EBP) beta and delta activate osteocalcin gene transcription and synergize with Runx2 at the C/EBP element to regulate bone-specific expression. J Biol Chem 277: 1316–1323.
29. Lin FT, Lane MD (1992) Antisense CCAAT/enhancer-binding protein RNA suppresses coordinate gene expression and triglyceride accumulation during differentiation of 3T3-L1 preadipocytes. Genes Dev 6: 533–544.
30. Lin FT, Lane MD (1994) CCAAT/enhancer binding protein alpha is sufficient to initiate the 3T3-L1 adipocyte differentiation program. Proc Natl Acad Sci U S A 91: 8757–8761.
31. Yeh WC, Cao Z, Classon M, McKnight SL (1995) Cascade regulation of terminal adipocyte differentiation by three members of the C/EBP family of leucine zipper proteins. Genes Dev 9: 168–181.
32. Komori T (2005) Regulation of skeletal development by the Runx family of transcription factors. J Cell Biochem 95: 445–453.
33. Takeda S, Bonnamy JP, Owen MJ, Ducy P, Karsenty G (2001) Continuous expression of Cbfa1 in nonhypertrophic chondrocytes uncovers its ability to induce hypertrophic chondrocyte differentiation and partially rescues Cbfa1-deficient mice. Genes Dev 15: 467–481.
34. Kronenberg HM (2006) PTHrP and skeletal development. Ann N Y Acad Sci 1068: 1–13.
35. Chikuda H, Kugimiya F, Hoshi K, Ikeda T, Ogasawara T, et al. (2004) Cyclic GMP-dependent protein kinase II is a molecular switch from proliferation to hypertrophic differentiation of chondrocytes. Genes Dev 18: 2418–2429.
36. Kawasaki Y, Kugimiya F, Chikuda H, Kamekura S, Ikeda T, et al. (2008) Phosphorylation of GSK-3beta by cGMP-dependent protein kinase II promotes hypertrophic differentiation of murine chondrocytes. J Clin Invest 118: 2506–2515.
37. Hata K, Nishimura R, Ueda M, Ikeda F, Matsubara T, et al. (2005) A CCAAT/enhancer binding protein beta isoform, liver-enriched inhibitory protein, regulates commitment of osteoblasts and adipocytes. Mol Cell Biol 25: 1971–1979.
38. MacLean HE, Guo J, Knight MC, Zhang P, Cobrinik D, et al. (2004) The cyclin-dependent kinase inhibitor p57(Kip2) mediates proliferative actions of PTHrP in chondrocytes. J Clin Invest 113: 1334–1343.
39. Guo J, Chung UI, Yang D, Karsenty G, Bringhurst FR, et al. (2006) PTH/PTHrP receptor delays chondrocyte hypertrophy via both Runx2-dependent and -independent pathways. Dev Biol 292: 116–128.
40. Pejchalova K, Krejci P, Wilcox WR (2007) C-natriuretic peptide: an important regulator of cartilage. Mol Genet Metab 92: 210–215.
41. Pfeifer A, Aszodi A, Seidler U, Ruth P, Hofmann F, et al. (1996) Intestinal secretory defects and dwarfism in mice lacking cGMP-dependent protein kinase II. Science 274: 2082–2086.
42. Zhao X, Zhuang S, Chen Y, Boss GR, Pilz RB (2005) Cyclic GMP-dependent protein kinase regulates CCAAT enhancer-binding protein beta functions through inhibition of glycogen synthase kinase-3. J Biol Chem 280: 32683–32692.
43. Schlossmann J, Hofmann F (2005) cGMP-dependent protein kinases in drug discovery. Drug Discov Today 10: 627–634.
44. Li H, Gade P, Xiao W, Kalvakolanu DV (2007) The interferon signaling network and transcription factor C/EBP-beta. Cell Mol Immunol 4: 407–418.
45. Takahashi K, Nakayama K, Nakayama K (2000) Mice lacking a CDK inhibitor, p57Kip2, exhibit skeletal abnormalities and growth retardation. J Biochem 127: 73–83.
46. Yan Y, Frisen J, Lee MH, Massague J, Barbacid M (1997) Ablation of the CDK inhibitor p57Kip2 results in increased apoptosis and delayed differentiation during mouse development. Genes Dev 11: 973–983.
47. Zhang P, Liegeois NJ, Wong C, Finegold M, Hou H, et al. (1997) Altered cell differentiation and proliferation in mice lacking p57KIP2 indicates a role in Beckwith-Wiedemann syndrome. Nature 387: 151–158.
48. Rossi F, MacLean HE, Yuan W, Francis RO, Semenova E, et al. (2002) p107 and p130 Coordinately regulate proliferation, Cbfa1 expression, and hypertrophic differentiation during endochondral bone development. Dev Biol 247: 271–285.
49. Reynaud EG, Pelpel K, Guillier M, Leibovitch MP, Leibovitch SA (1999) p57(Kip2) stabilizes the MyoD protein by inhibiting cyclin E-Cdk2 kinase activity in growing myoblasts. Mol Cell Biol 19: 7621–7629.
50. Imamura T, Imamura C, Iwamoto Y, Sandell LJ (2005) Transcriptional co-activators CREB-binding protein/p300 increase chondrocyte Cd-rap gene expression by multiple mechanisms including sequestration of the repressor CCAAT/enhancer-binding protein. J Biol Chem 280: 16625–16634.
51. Imamura T, Imamura C, McAlinden A, Davies SR, Iwamoto Y, et al. (2008) A novel tumor necrosis factor alpha-responsive CCAAT/enhancer binding protein site regulates expression of the cartilage-derived retinoic acid-sensitive protein gene in cartilage. Arthritis Rheum 58: 1366–1376.
52. Okazaki K, Yu H, Davies SR, Imamura T, Sandell LJ (2006) A promoter element of the CD-RAP gene is required for repression of gene expression in non-cartilage tissues in vitro and in vivo. J Cell Biochem 97: 857–868.
53. Massaad C, Paradon M, Jacques C, Salvat C, Bereziat G, et al. (2000) Induction of secreted type IIA phospholipase A2 gene transcription by interleukin-1beta. Role of C/EBP factors. J Biol Chem 275: 22686–22694.
54. Thomas B, Berenbaum F, Humbert L, Bian H, Bereziat G, et al. (2000) Critical role of C/EBPdelta and C/EBPbeta factors in the stimulation of the cyclooxygenase-2 gene transcription by interleukin-1beta in articular chondrocytes. Eur J Biochem 267: 6798–6809.
55. Mizui Y, Yamazaki K, Kuboi Y, Sagane K, Tanaka I (2000) Characterization of 5′-flanking region of human aggrecanase-1 (ADAMTS4) gene. Mol Biol Rep 27: 167–173.
56. Raymond L, Eck S, Mollmark J, Hays E, Tomek I, et al. (2006) Interleukin-1 beta induction of matrix metalloproteinase-1 transcription in chondrocytes requires ERK-dependent activation of CCAAT enhancer-binding protein-beta. J Cell Physiol 207: 683–688.

57. Yano F, Kugimiya F, Ohba S, Ikeda T, Chikuda H, et al. (2005) The canonical Wnt signaling pathway promotes chondrocyte differentiation in a Sox9-dependent manner. Biochem Biophys Res Commun 333: 1300–1308.
58. Morita S, Kojima T, Kitamura T (2000) Plat-E: an efficient and stable system for transient packaging of retroviruses. Gene Ther 7: 1063–1066.
59. Kawasaki H, Taira K (2003) Short hairpin type of dsRNAs that are controlled by tRNA(Val) promoter significantly induce RNAi-mediated gene silencing in the cytoplasm of human cells. Nucleic Acids Res 31: 700–707.

Osteoarthritis and Cartilage (2009) ■■, ■■■–■■■

doi:10.1016/j.joca.2009.02.003

Osteoarthritis and Cartilage | ICRS International Cartilage Repair Society | OARSI OSTEOARTHRITIS RESEARCH SOCIETY INTERNATIONAL

Transcriptional induction of SOX9 by NF-κB family member RelA in chondrogenic cells

M. Ushita†, T. Saito†, T. Ikeda‡, F. Yano§, A. Higashikawa†, N. Ogata‡, U. Chung§, K. Nakamura† and H. Kawaguchi†*

† *Department of Sensory & Motor System Medicine, University of Tokyo, Hongo 7-3-1, Bunkyo-ku, Tokyo 113-8655, Japan*

‡ *Department of Bone and Cartilage Regenerative Medicine, University of Tokyo, Hongo 7-3-1, Bunkyo-ku, Tokyo 113-8655, Japan*

§ *Center for Disease Biology and Integrative Medicine, University of Tokyo, Hongo 7-3-1, Bunkyo-ku, Tokyo 113-8655, Japan*

Summary

Objective: Although SOX9 is a key molecule for chondrogenic differentiation, little is known about the upstream signal. The present study attempted to identify transcription factors to induce SOX9 expression and examined the mechanism.

Methods: Sequences of about 1 kb of 5′-end flanking regions were compared between human and mouse SOX9 genes. *In vivo* localization was examined by immunohistochemistry in the limb cartilage of fetal mice. Promoter activities of the SOX9, SOX6, and type II collagen (COL2A1) genes were determined in human non-chondrogenic HeLa cells and mouse chondrogenic ATDC5 cells transfected with a luciferase-reporter gene containing the promoter fragments. Protein–DNA binding was examined by electrophoretic mobility shift and chromatin immunoprecipitation assays. The chondrogenic differentiation was assessed by endogenous SOX9, SOX6, and COL2A1 mRNA levels, and by Alcian blue staining and alkaline phosphatase activity.

Results: Among transcription factors whose binding motifs were identified in the highly-conserved regions between human and mouse SOX9 promoters, a nuclear factor kappa B (NF-κB) member RelA strongly activated the promoter activity. RelA and SOX9 were co-localized in the limb cartilage. Deletion, mutagenesis, and tandem-repeat analyses identified the core region responsive to RelA at the NF-κB binding motif to be around −250 bp of the human SOX9 promoter, and this was confirmed to show specific binding to RelA. RelA induced the chondrogenic differentiation parameters in HeLa and ATDC5 cells.

Conclusion: We have identified RelA as a transcriptional factor for SOX9 induction and chondrogenic differentiation *via* binding to an NF-κB binding motif in the SOX9 promoter.

Keywords: SOX9, RelA, Chondrocyte, Transcription.

Introduction

Skeletal development is initiated by the recruitment of undifferentiated mesenchymal cells into condensations, which differentiate into pre-chondrocytes and then chondrocytes that produce cartilage-specific extracellular matrix proteins like type II collagen (COL2A1)[1]. Sex-determining region Y-type high mobility group box 9 (SOX9) is expressed in the mesenchymal cells, pre-chondrocytes and chondrocytes[2,3], and functions as a master transcriptional activator of COL2A1 and other chondrocyte-specific matrix proteins, in cooperation with the co-factors SOX6 and L-SOX5[4–9]. Expressions of the SOX6 and L-SOX5 are also controlled by SOX9[4,10]. Studies in mice have shown that SOX9 is essential for multiple steps in the chondrogenic differentiation pathway: conditional ablation of the SOX9 gene in the limb buds before mesenchymal condensation resulted in a complete absence of chondrocytes, whereas the conditional ablation after mesenchymal condensation resulted in a severe generalized chondrodysplasia[10–12]. In humans as well, heterozygous mutations of the SOX9 gene cause a severe chondrodysplasia, known as campomelic dysplasia[11,13]. Furthermore, we previously reported that SOX9 in combination with SOX6 and L-SOX5 (the SOX trio) stimulated chondrogenesis even from non-chondrogenic cells of mouse and human origins, implicating a possible clinical application of this signal to cartilage regeneration[14]. Despite the substantial information about the expression profiles and the target genes of SOX9, little is known about the upstream signaling or the functional regulation of the SOX9 promoter. To identify transcription factors that induce SOX9 expression, the present study initially compared the genomic sequences of proximal promoter regions between human and mouse SOX9 genes, and identified several highly-conserved regions containing putative transcription

*Address correspondence and reprint requests to: Dr Hiroshi Kawaguchi, Department of Sensory & Motor System Medicine, Faculty of Medicine, University of Tokyo, Hongo 7-3-1, Bunkyo, Tokyo 113-8655, Japan. Tel: 81-3-3815-5411 ext. 30473; Fax: 81-3-3818-4082; E-mail: kawaguchi-ort@h.u-tokyo.ac.jp

Received 6 October 2008; revision accepted 11 February 2009.

Please cite this article in press as: Ushita M et al., Transcriptional induction of SOX9 by NF-κB family member RelA in chondrogenic cells, Osteoarthritis Cartilage (2009), doi:10.1016/j.joca.2009.02.003

factor-binding motifs. Among the candidate transcription factors, our further analyses found that nuclear factor kappa B (NF-κB) family member RelA (NF-κB p65) most strongly activated the human SOX9 promoter activity.

The NF-κB family of transcription factors plays a crucial role in a broad range of biological processes, including immune responses, inflammation, proliferation, differentiation and apoptosis[15–17]. The family includes RelA, RelB, Rel, p105/p50 and p100/p52, each of which contains a Rel homology domain that mediates DNA binding and dimerization. Numerous studies have established that IκB proteins are phosphorylated and degraded by a large protein complex IκB kinase (IKK) in response to several signals, thereby allowing free NF-κB complexes to translocate from the cytoplasm into the nucleus, leading to target gene transactivation[18,19]. The NF-κB family genes are expressed in the chick limb cartilage, and the blockage of the NF-κB activity caused the arrest of the limb outgrowth[20]. The IKKα-deficient mice also exhibited suppression of limb outgrowth[21,22]. Since these lines of evidence implicate the interaction between NF-κB and SOX9 signals during skeletal development, the present study investigated the mechanism underlying the transcriptional regulation of the SOX9 promoter by RelA.

Materials and methods

COMPARISON OF THE PROXIMAL PROMOTER SEQUENCES OF THE HUMAN, MOUSE AND CHICK SOX9 GENES

We compared the sequences of the 5′-end flanking regions relative to the transcription start site among 4 kb human, 4 kb mouse and 300 bp chick SOX9 gene, using BLASTN search[23]. The detected sequences were aligned by the Vector-NTI software (Invitrogen), and the transcription factor-binding motifs were predicted using the TFSEARCH web site (Computational Biology Research Center, AIST, Japan).

CELL CULTURES

The human epithelial cell line HeLa (RIKEN Cell Bank, Tsukuba, Japan) was cultured in high-glucose Dulbecco's modified Eagle's medium (DMEM) with 10% fetal bovine serum (FBS). Mouse chondrogenic ATDC5 cells (RIKEN Cell Bank) were grown and maintained in DMEM/F12 (1:1) with 5% FBS. To induce chondrogenic differentiation, ATDC5 cells were cultured in the presence of insulin-transferring-sodium selenite media supplement (ITS) (Sigma) for 3 weeks and replaced by αMEM/5% FBS with 4 mM inorganic phosphate (Pi) for 2 d[24].

CONSTRUCTION OF EXPRESSION VECTORS

Full-length human cDNA sequences of the transcription factors were polymerase chain reaction (PCR)-amplified and cloned into pCMV-HA vector (Clontech, Palo Alto, CA, USA). The Gene Bank access numbers are as follows: NFAT1 NM_012340.3, NFAT2 NM_006162.3, NFAT3 NM_004554.4, NFAT4 NM_004555.2, NFAT5 NM_138714, Fos NM_005252.2, Jun NM_002228.3, Fra-1 NM_005438.3, RelA NM_021975.2, RelB NM_006509.2, Rel NM_002908.2, p105 NM_003998.2, p100 NM_001077493.1, ATF1 NM_005171.3, ATF2 NM_001880.2, ATF4 NM_001675.2, ATF6 NM_007348.2, ATF7 NM_001130059.1, CREB NM_004379.2, C/EBPα NM_004364.2, C/EBPβ NM_005194.2, C/EBPδ NM_005195.3, C/EBPε NM_001805.2, GATA-1 NM_ 002049.3, GATA-2 NM_032638.3, GATA-3 NM_001002295.1, GATA-4 NM_002052.3, GATA-5 NM_080473.4, GATA-6 NM_005257.3. The primer sequences are available upon request.

LUCIFERASE ASSAY

The human SOX9 promoter region from −927 to +84 bp relative to the transcriptional start site (TSS) was obtained by PCR using human genomic DNA as a template and were cloned into the EcoRI and HindIII sites of the modified pGL3 vector containing additional cloning sites between the XhoI and HindIII sites of the original plasmid, the pGL3-basic vector (Promega, Madison, WI, USA). Deletion and mutation constructs were created by PCR technique. Tandem-repeat constructs were created by ligating the double strand oligonucleotides into EcoRI site of the modified pGL3 vector. Transfection of HeLa and ATDC5 cells was performed in quadruplicate in 48-well plates using FuGENE 6 transfection reagent (Roche, Mannheim, Germany): FuGENE 6 with a total amount of 150 ng of plasmid DNA, 100 ng of pGL3 reporter vector, 50 ng of effector vector, and 4 ng of pRL-TK vector (Promega) for internal control per well. Cells were harvested 48 h after the transfection. The luciferase assay was performed with a dual-luciferase-reporter assay system (Promega) using a GloMax 96 Microplate Luminometer (Promega). The results were shown as the ratio of the firefly activities to the renilla activities. For the SOX6 promoter assay, a luciferase-reporter construct containing the human SOX6 promoter and exon 1 region (−517 to IVS1 + 23) was generated and transfected in HeLa and ATDC5 cells as reported previously[25]. For the COL2A1 promoter assay, a luciferase-reporter construct containing the four repeats of the 49 bp SOX9 enhancer and the basal promoter (from −183 to +23) in the human COL2A1 gene was generated and transfected in the cells[26].

IMMUNOHISTOCHEMISTRY

Tissues from C57BL6 mouse embryos (E17.5) were fixed in 4% paraformaldehyde/phosphate-buffered saline (PBS) overnight at 4°C, embedded in paraffin and cut into 5 μm sections. Sections were incubated overnight at 4°C with primary antibodies to RelA (C-20) (1:200; Santa Cruz Biotechnology, Santa Cruz, CA, USA) and SOX9 (1:500; Santa Cruz Biotechnology), as well as the non-immune serum as the control. The localizations were detected with horseradish peroxidase-conjugated secondary antibodies (Promega, Madison, WI, USA).

ELECTROPHORETIC MOBILITY SHIFT ASSAY (EMSA)

RelA protein was prepared by *in vitro* translation using the TNT T7 Coupled Reticulocyte Lysate System (Promega) and pCITE4 vector (Novagen, Milwaukee, WI, USA) into which RelA complementary DNA was cloned. The translation product was verified by Western blotting. Nuclear extracts were prepared from undifferentiated and differentiated ATDC5 cells before and after the culture with ITS for 3 weeks and Pi for 2 d, respectively. EMSA was carried out using a DIG gel shift kit (Roche, Mannheim, Germany) according to the manufacturer's instructions. Binding reactions were incubated for 30 min at room temperature. For competition analyses, 100-fold excess of unlabeled competitor probe was included in the binding reaction. For the supershift experiments, 1 μL of the antibody to RelA (C-20) above was added after 30 min of the binding reaction, and the reaction was incubated for an additional 30 min at room temperature. Samples were loaded onto Novex 6% TBE gels (Invitrogen), and electrophoresed at 100 V for 60 min.

CHROMATIN IMMUNOPRECIPITATION (ChIP) ASSAY

The ChIP assay was performed with a OneDay ChIP kit (Diagenode, Liege, Belgium) according to the manufacturer's instructions. *In vivo* cross-linking was performed 2 d after the transfection of HeLa cells with EV, RelA using FuGENE 6, and then the lysates were sonicated to shear genomic DNA. For immunoprecipitation, an antibody to RelA and the control normal rabbit immunoglobulin G (IgG) were used. Two primer sets, one spanning (−478/−239 bp) and the other not spanning (−3781/−3625 bp) the identified NF-κB motif, were employed. PCR was performed using Ex Taq (Takara Bio, Otsu, Japan) in the presence of 10% dimethyl sulfoxide.

GENE TRANSFER

For transient gene transfer, 2×10^5 HeLa cells were cultured in 6-well plates to subconfluency, and transfected with 1 μg of expression vector of RelA or the control empty vector (EV) using FuGENE 6. After 48 h, total mRNA of harvested cells was extracted and analyzed by real-time RT-PCR as described below.

Production of retroviral vectors was performed as described previously[27]. For retroviral gene transfer, 2×10^6 Plat-E cells were plated in 6-well plates, transfected with 2 μg pMx vector of RelA or the control green fluorescent protein (GFP) using FuGENE 6, and the conditioned medium was collected after 48 h. On the day before retroviral transfection, 3×10^5 of ATDC5 cells were plated onto a 60-mm culture dish. For the transfection, 4 mL of the conditioned medium containing the retrovirus was added to the cells with 32 μg of polybrene. Selection of the retrovirus-introduced cells was started 48 h after transfection in the medium containing 10 μg/mL of blasticidin.

REAL-TIME RT-PCR

Total RNA from cells was isolated with an RNeasy Mini kit (Qiagen, Hilden, Germany) according to the manufacturer's instructions, and an aliquot (1 μg) was reverse-transcribed with QuantiTect Reverse Transcription (Qiagen) to make single-stranded cDNA. Real-time RT-PCR was performed with an ABI Prism 7000 Sequence Detection System (Applied Biosystems, Foster City, CA, USA) using QuantiTect SYBR Green PCR Master Mix (Qiagen)

Please cite this article in press as: Ushita M et al., Transcriptional induction of SOX9 by NF-κB family member RelA in chondrogenic cells, Osteoarthritis Cartilage (2009), doi:10.1016/j.joca.2009.02.003

according to the manufacturer's instructions. Standard plasmids were synthesized with a TOPO TA Cloning kit (Invitrogen, Carlsbad, CA, USA), according to the manufacturer's instructions. All reactions were run in quadruplicate. Copy numbers of target gene messenger RNA (mRNA) in each total RNA were calculated by reference to standard curves and were adjusted to the human or mouse standard total RNA (ABI) with the human GAPDH or rodent GAPDH as an internal control. The primer sequences are available upon request.

CHONDROCYTE DIFFERENTIATION ASSAYS

For the Alcian blue staining, the cells were fixed with 10% (vol/vol) formaldehyde, and stained with 0.3% Alcian blue 8GS (Fluka, Buchs, Switzerland) in 0.1 N HCl. Alkaline phosphatase (ALP) staining was performed by a solution containing 0.01% naphtol AS-MX phosphate disodium salt, 1% *N,N*-dimethyl-formamide and 0.06% fast blue BB (Sigma). ALP activity was measured with a Lab Assay ALP kit (Wako, Osaka, Japan).

Results

IDENTIFICATION OF TRANSACTIVATORS OF THE SOX9 PROMOTER BY COMPARISON BETWEEN HUMAN AND MOUSE GENES

To identify transcription factors that activate the SOX9 promoter, we initially performed exhaustive comparison of the sequences of about 4 kb of the 5′-end flanking regions between human and mouse genes, and found that the 1.0 kb upstream of the TSS was about 80% conserved between the species. The sequence search identified the binding motifs of NFAT, AP-1, NF-κB, Sp1, CREB/ATF, CCAAT, and GATA in the highly-conserved regions (Fig. 1). The sequence of the motifs at the proximal region showed good conservation in the chick gene as well as in the human and mouse ones.

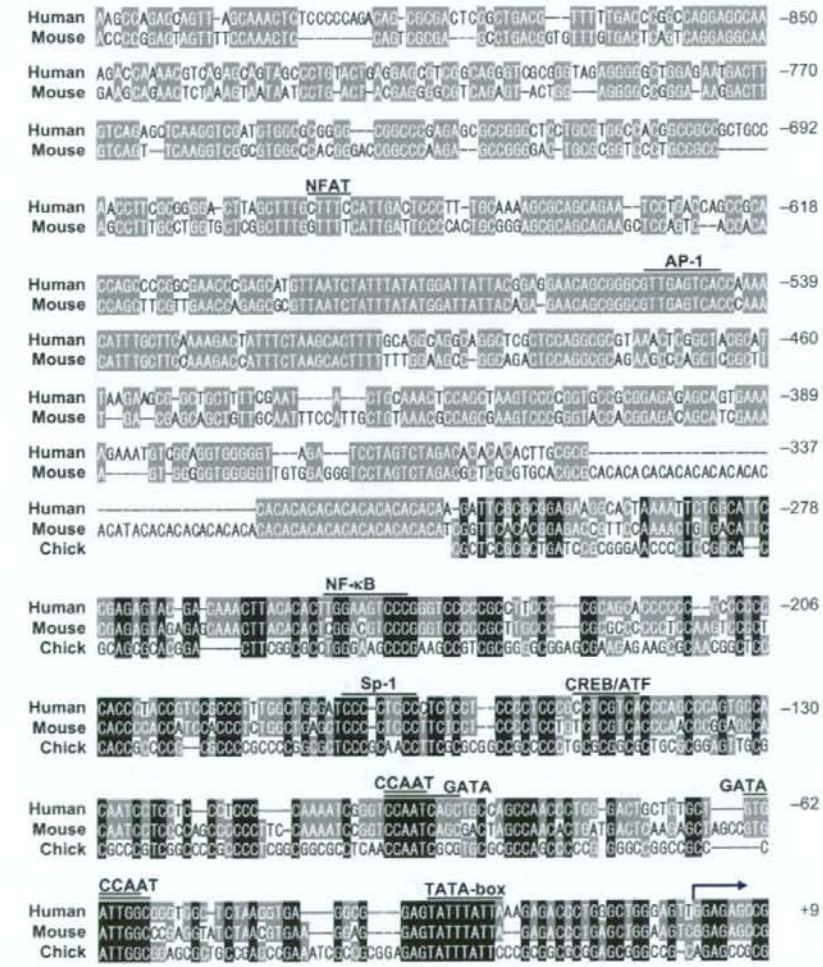

Fig. 1. Comparison of the proximal promoter sequences of the human, mouse and chick SOX9 genes. Conserved nucleotides in the two or three species are denoted by white letters shaded in gray or black, respectively. An arrow shows the transcription start sites of the human and mouse genes. Putative binding motifs of transcription factors identified in highly-conserved regions are indicated.

Please cite this article in press as: Ushita M et al., Transcriptional induction of SOX9 by NF-κB family member RelA in chondrogenic cells, Osteoarthritis Cartilage (2009), doi:10.1016/j.joca.2009.02.003

We therefore created expression vectors of the transcription factors whose binding motifs were identified: NFAT1, NFAT2, NFAT3, NFAT4, NFAT5, Fos, Jun, Fra-1, RelA, RelB, Rel, p105, p50, p100, p52, ATF1, ATF2, ATF4, ATF6, ATF7, CREB, C/EBPα, C/EBPβ, C/EBPδ, C/EBPε, GATA-1, GATA-2, GATA-3, GATA-4, GATA-5, and GATA-6; and transfected them in human non-chondrogenic HeLa cells and mouse chondrogenic ATDC5 cells with a luciferase-reporter construct containing the 5′-end flanking region (−927/+84) of the human SOX9 gene (Fig. 2). Among the transcription factors, the luciferase-reporter assay revealed that an NF-κB family member RelA strongly activated the SOX9 promoter activity in both HeLa and ATDC5 cells, causing us to speculate that RelA is a potent transcriptional factor for SOX9 induction.

IN VIVO LOCALIZATION OF RelA AND SOX9 IN THE LIMB CARTILAGE

To know the possible interaction between RelA and SOX9 *in vivo*, we then examined the expression patterns of RelA and SOX9 in the limb cartilage of fetal mice (Fig. 3). Both RelA and SOX9 were well co-localized in resting chondrocytes, as well as in pre-hypertrophic and hypertrophic chondrocytes, suggesting the molecular interaction between RelA and SOX9 during the chondrocyte differentiation.

IDENTIFICATION OF THE CORE REGION RESPONSIVE TO RelA IN THE SOX9 PROXIMAL PROMOTER

To identify the region responsive to RelA in the human SOX9 proximal promoter, we performed the deletion analysis of the luciferase assay in HeLa and ATDC5 cells

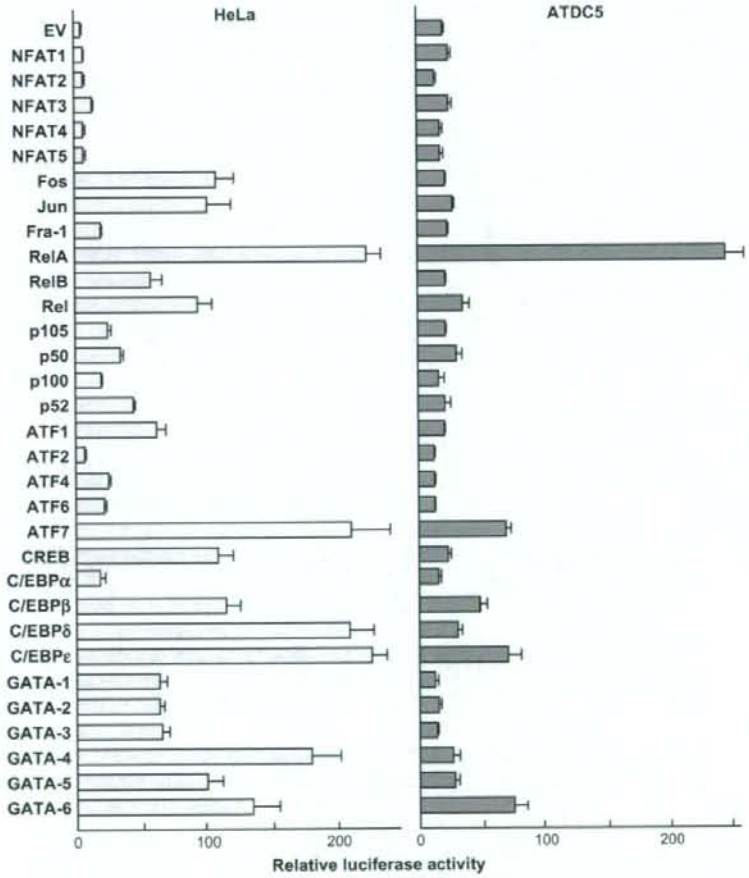

Fig. 2. Luciferase assay for the human SOX9 promoter activity by the transcription factors whose binding motifs were identified in Fig. 1. Human non-chondrogenic HeLa cells and mouse chondrogenic ATDC5 cells co-transfected with luciferase-reporter constructs containing the proximal 5′-end flanking region (from −927 to +84 bp relative to the TSS) of the human SOX9 gene, and the effecter vectors or the control EV. Data are shown as means (bars) ± S.E.M. (error bars) of relative luciferase activity (the ratio of the firefly activities to the renilla activities) for 4 wells/group.

Please cite this article in press as: Ushita M et al., Transcriptional induction of SOX9 by NF-κB family member RelA in chondrogenic cells, Osteoarthritis Cartilage (2009), doi:10.1016/j.joca.2009.02.003

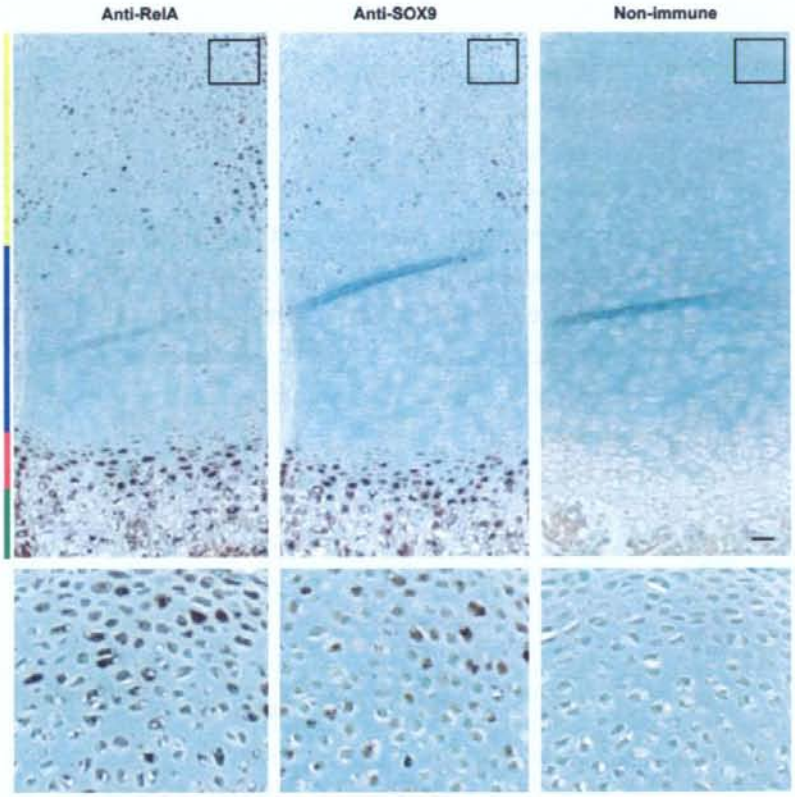

Fig. 3. Localizations of RelA and SOX9 by immunohistochemistry using the antibodies and the control non-immune serum in the proximal tibial limb cartilage of fetal mice (E17.5). Inset boxes in the top panels indicate the regions of the respective lower figures. Yellow, blue, red and green bars to the left of the panels indicate layers of resting, proliferative, pre-hypertrophic and hypertrophic zones, respectively. Scale bar, 100 μm.

co-transfected with RelA or the control EV. A series of 5′-deletions of the −927/+84 fragment identified the decreases of the transcriptional activity between −289 and −202 bp, and between −202 and −127 bp in both cells [Fig. 4(A)]. When we further compared the luciferase activity of the tandem repeats of the distal (−289/−203 bp) and proximal (−202/−128 bp) elements, only the distal responded to RelA in the repeat number-dependent manner, indicating that the region between −289 and −203 bp contains a core region responsive to RelA [Fig. 4(B)]. In fact, the identified −289/−203 bp element contained a consensus sequence of the NF-κB binding motif (HGGARNYYCC) at −252/−243 bp (TGGAAGTCCC), which was the only fully-matched sequence in the 1 kb SOX9 promoter.

We therefore prepared the 39 bp (−266/−228 bp) element containing the NF-κB motif for further analyses [Fig. 5(A)]. To examine the core responsive region in the element, we created two base mutations within the NF-κB binding motif, and further performed luciferase assay of tandem repeats of the wild-type and mutated elements in HeLa and ATDC5 cells. The repeat number-dependent transactivation of the wild-type element by RelA was suppressed by the mutagenesis in both cell types, confirming that the NF-κB binding motif is the core region responsive to RelA [Fig. 5(A)].

EMSA revealed the complex formation of the *in vitro*-translated RelA protein with the 39 bp element above [Fig. 5(B), lane 2]. Mutagenesis analyses in the element showed that the complex formation was abolished by mutations inside the NF-κB motif (m1 and m2), but not by outside mutations (m3) [Fig. 5(B), lanes 3–5]. Cold competition with excess amount of the unlabeled wild-type and outside mutation probes suppressed the complex formation, while that with the unlabeled inside mutation probes did not affect it [Fig. 5(B), lanes 6–9]. The binding between RelA and the NF-κB motif was confirmed by the complex formation of the 39 bp probe with nuclear extracts from ATDC5 cells. Interestingly, the complex formation was stronger by nuclear extracts from differentiated ATDC5 cells after the culture with differentiation medium than those of undifferentiated cells before the culture [Fig. 5(B), lanes 14 and 15]. Both complexes with the *in vitro*-translated RelA protein [Fig. 5(B), lane 12] and the ATDC5 nuclear extracts [Fig. 5(B), lane 18] underwent supershifts by addition of an antibody to RelA. These results demonstrate the specific binding between RelA and the NF-κB motif in the SOX9 promoter.

Please cite this article in press as: Ushita M et al., Transcriptional induction of SOX9 by NF-κB family member RelA in chondrogenic cells, Osteoarthritis Cartilage (2009), doi:10.1016/j.joca.2009.02.003

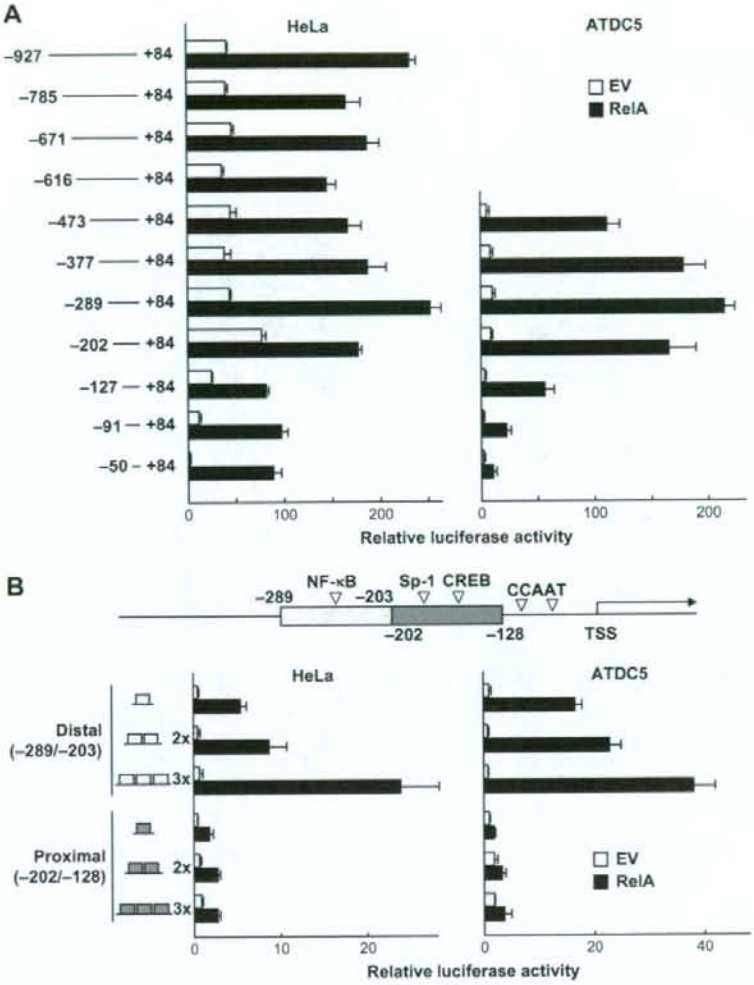

Fig. 4. (A) Identification of the region responsive to RelA by the deletion analysis of the luciferase assay in HeLa and ATDC5 cells. The cells with luciferase-reporter constructs containing the abovementioned −927/+84 region of the human SOX9 gene and the series of deletion fragments were co-transfected with RelA or the control EV. (B) Luciferase assays of the tandem repeats of the distal (−289/−203 bp relative to the TSS) and proximal (−202/−128 bp) elements that were identified in the deletion analysis above in HeLa and ATDC5 cells co-transfected with RelA or the control EV. The loci of consensus binding motifs that were identified by the present and previous studies (NF-κB, Sp1, CREB, and CCAAT) are indicated by open arrowheads. Data are shown as means (bars) ± S.E.M. (error bars) of relative luciferase activity for 4 wells/group.

ChIP assay showed the *in vivo* binding of RelA with the SOX9 promoter including the NF-κB motif [Fig. 5(C), left]. The specificity of the binding was confirmed because it was not immunoprecipitated by the non-immune IgG [Fig. 5(C), left], and no amplification was seen with a primer set that does not span the NF-κB motif [Fig. 5(C), right].

FUNCTIONAL ROLE OF RelA IN CHONDROGENIC DIFFERENTIATION

Finally, we investigated the involvement of RelA in chondrogenic differentiation. Among the NF-κB family members transfected in HeLa cells and ATDC5 cells, luciferase assays revealed that RelA transfection strongly stimulated the promoter activities of SOX6 and COL2A1, the representative chondrogenic markers besides SOX9 [Fig. 6(A)].

When RelA or the control EV was transiently transfected into HeLa cells, the RelA overexpression stimulated the mRNA levels of endogenous SOX9, SOX6, and COL2A1 [Fig. 6(B)]. To further investigate the function of RelA in chondrogenic differentiation, we established stable lines of ATDC5 cells with retroviral overexpression of RelA or the control GFP vector, and cultured them in the chondrogenic

Please cite this article in press as: Ushita M et al., Transcriptional induction of SOX9 by NF-κB family member RelA in chondrogenic cells, Osteoarthritis Cartilage (2009), doi:10.1016/j.joca.2009.02.003

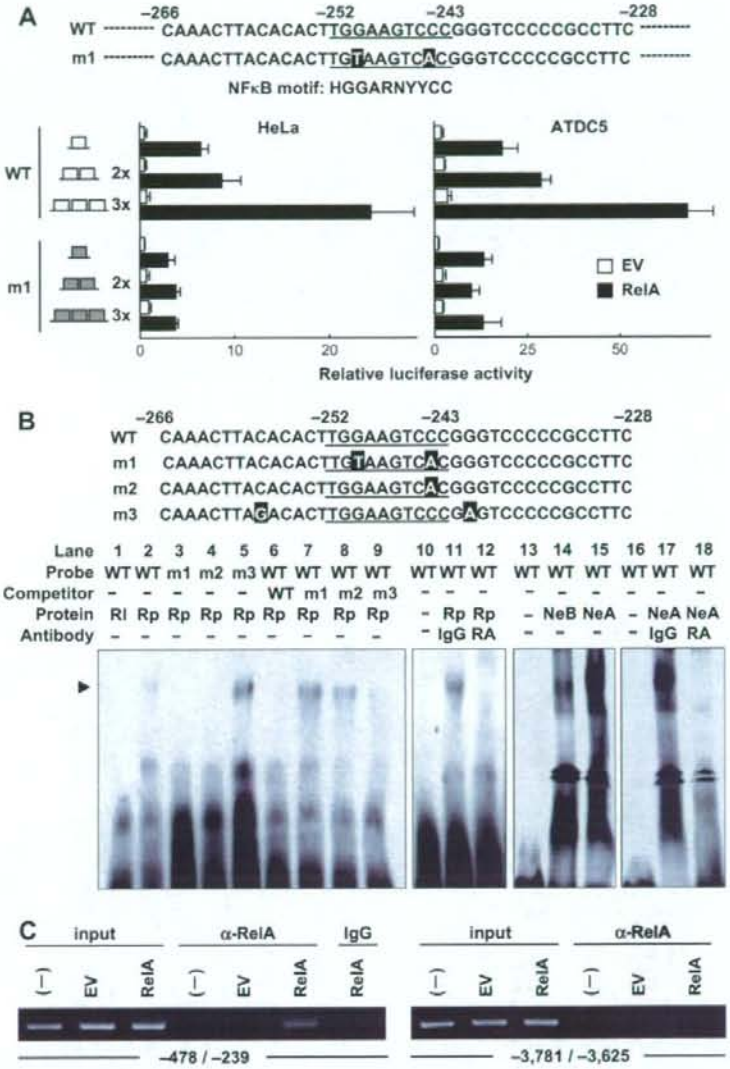

Fig. 5. (A) The 39 bp element (−265/−227 bp) containing the putative NF-κB motif (−251/−242 bp, underlined) in the identified region (wild-type; WT) and that with two base mutations at −243 and −249 bp (black boxes) within the NF-κB motif (m1). Luciferase assays of the tandem repeats of the WT and m1 elements in HeLa and ATDC5 cells co-transfected with RelA or the control EV. Data are shown as means (bars) ± S.E.M. (error bars) of relative luciferase activity for 4 wells/group. (B) EMSA for binding of the *in vitro*-translated RelA protein (Rp; lanes 1–12) or nuclear extract (Ne; lanes 13–18) with the WT or the mutated probes of the 39 bp element (−265/−227 bp) above. RI denotes reticulocyte lysate without the transcriptional/translational template. Mutations were created inside (m1 for double mutations and m2 for a single mutation) and outside (m3) the NF-κB motif. Cold competition with 100-fold excess of unlabeled WT or the mutated probes is also presented. Binding to the probe was compared between nuclear extracts of ATDC5 cells before (NeB) and after (NeA) the chondrogenic differentiation by ITS and Pi. The arrowhead indicates the shifted bands of the RelA–DNA probe complex. RA and IgG denote an antibody to RelA and non-immune IgG as the control, respectively. (C) ChIP assay for specific binding of RelA to the NF-κB motif. Cell lysates of HeLa cells with no transfection (−), transfected with EV, or RelA were amplified by a primer set spanning the NF-κB motif (−478/−239 bp, left panel) or not spanning the motif (−3781/−3625 bp, right panel) before (input) and after immunoprecipitation with an antibody to RelA (α-RelA) or the control non-immune IgG (α-IgG).

Please cite this article in press as: Ushita M et al., Transcriptional induction of SOX9 by NF-κB family member RelA in chondrogenic cells, Osteoarthritis Cartilage (2009), doi:10.1016/j.joca.2009.02.003